

**DYNAMIC HEART RATE MEASUREMENTS FROM VIDEO
SEQUENCES USING CANONICAL COMPONENT ANALYSIS**

LING SIONG SHI

**DISSERTATION SUBMITTED IN FULFILMENT OF THE
REQUIREMENTS FOR THE DEGREE OF MASTER OF
ENGINEERING SCIENCE**

**FACULTY OF ENGINEERING
UNIVERSITY OF MALAYA
KUALA LUMPUR**

2019

UNIVERSITY OF MALAYA
ORIGINAL LITERARY WORK DECLARATION

Name of Candidate: Ling Siong Shi

Matric No: KGA150001

Name of Degree: Master of Engineering Science

Title of Project Paper/Research Report/Dissertation/Thesis ("this Work"):

Dynamic Heart Rate Measurements from Video Sequences using Canonical
Component Analysis

Field of Study: Signal and Systems

I do solemnly and sincerely declare that:

- (1) I am the sole author/writer of this Work;
- (2) This Work is original;
- (3) Any use of any work in which copyright exists was done by way of fair dealing and for permitted purposes and any excerpt or extract from, or reference to or reproduction of any copyright work has been disclosed expressly and sufficiently and the title of the Work and its authorship have been acknowledged in this Work;
- (4) I do not have any actual knowledge nor do I ought reasonably to know that the making of this work constitutes an infringement of any copyright work;
- (5) I hereby assign all and every rights in the copyright to this Work to the University of Malaya ("UM"), who henceforth shall be owner of the copyright in this Work and that any reproduction or use in any form or by any means whatsoever is prohibited without the written consent of UM having been first had and obtained;
- (6) I am fully aware that if in the course of making this Work I have infringed any copyright whether intentionally or otherwise, I may be subject to legal action or any other action as may be determined by UM.

Candidate's Signature

Date:

Subscribed and solemnly declared before,

Witness's Signature

Date:

Name:

Designation:

ABSTRACT

Video images have been widely used to extract relevant information for applications. One such application is the heart rate estimation using facial images from video sequences. A method using Canonical Component Analysis (CCA) is introduced to estimate the heart rate reading. In this study, two five-second video is used. The starting points of the two 5-second video frames are not the same. One of them starts one second later. It is assumed that these two 5-second video frames will contain the heart rate signals that are strongly correlated to each other and the random artifacts and noises appearing in both video frames are not correlated to each other. Therefore the desired heart rate will remain unchanged which have the ability to give maximum correlation values. The obtained eigenvalues and eigenvectors with maximum correlation values now can be used to find the desired original sources. By examining the most correlated signal within these two video frames using Canonical Component Analysis (CCA), the heart rate can be estimated. The identified heart signal from the result of CCA is then passed to a bandpass filter (0.8-4Hz) followed by Fast Fourier Transform to obtain the heart rate. Two experiments which involve increasing and decreasing dynamic heart rate were conducted. For both experiments, eight subjects took part in a cycling activity and their heart rates varied from 70 to 157 beats per minute (BPM). The results from both methods showed that acceptable average error rates of less than 3.70 BPM are observed between the actual and the estimated heart rates. In addition to that, a study was carried out to determine the minimum distance between the subject and video camera with fixed video duration. The results from this experiment showed acceptable error rates are observed when the distance between them is less than 130cm. In the last experiment, the effects of varying video duration but with fixed distance are carried out. Acceptable error rates are observed between the actual and estimated video duration greater than 6 seconds.

ABSTRAK

Banyak aplikasi telah menggunakan imej video untuk mendapatkan maklumat yang relevan. Salah satu aplikasi sedemikian ialah anggaran kadar denyutan dengan menggunakan imej muka dari video. Satu kaedah yang menggunakan Analisis Komponen Berkanun (CCA) diperkenalkan untuk menganggarkan bacaan kadar jantung. Dalam kajian ini, dua video lima saat akan digunakan. Titik permulaan dari dua bingkai video 5 saat tidak sama. Salah seorang daripada mereka bermula satu saat kemudian. Adalah diandaikan bahawa kedua-dua bingkai video 5 saat ini akan mengandungi isyarat denyutan jantung yang sangat berkaitan dengan satu sama lain dan artifak dan bunyi rawak yang muncul dalam kedua-dua bingkai video tidak berkorelasi antara satu sama lain. Oleh itu kadar denyutan yang diinginkan akan kekal tidak berubah yang mempunyai kemampuan untuk memberikan nilai korelasi maksimum. Nilai eigen yang diperoleh dan vektor eigen yang mempunyai nilai korelasi maksimum kini boleh digunakan untuk mencari sumber asli yang dikehendaki. Dengan memeriksa isyarat yang paling berkorelasi dalam kedua-dua bingkai video ini menggunakan CCA, kadar denyutan jantung boleh dianggarkan. Isyarat jantung yang dikenal pasti dari hasil CCA kemudiannya dihantar ke penapis bandpass (0.8-4Hz) diikuti dengan transformasi fourier cepat untuk mendapatkan kadar denyutan jantung. Dua eksperimen melibatkan kadar denyutan dinamik yang meningkat dan menurun telah dijalankan. Dalam kedua-dua eksperimen ini, lapan subjek diminta mengambil bahagian dalam aktiviti berbasikal dan kadar jantungnya berbeza dari 70 hingga 157 beats per minit (BPM). Keputusan dari kedua-dua kaedah menunjukkan bahawa kadar ralat purata kurang daripada 3.70 BPM antara kadar jantung sebenar dengan anggaran kadar jantung. Di samping itu, satu kajian telah dijalankan untuk menentukan jarak minimum antara subjek dan kamera video dengan tempoh video yang tetap. Hasil dari eksperimen ini menunjukkan bahawa kadar ralat boleh didapatkan apabila jarak di antara mereka kurang dari 130cm. Dalam

eksperimen lepas, kesan jangka masa video yang berbeza-beza dengan jarak yang tetap telah dijalankan. Kadar kesilapan yang boleh diterima diperhatikan di antara sebenar dan anggaran untuk tempoh video yang melebihi 6 saat.

University of Malaya

ACKNOWLEDGMENTS

Firstly, I would like to express my sincere gratitude to my supervisor Prof. Dr. P. Raveendran for the continuous support of my master study and related research. His guidance helped me in all the time of research and writing of this thesis. I could not have imagined having a better supervisor and mentor for my master study.

I thank my colleagues for the stimulating discussions. In particular, I am grateful to Dr. Lim Chern Loon and Dr. Yu Yong Poh for providing technical knowledge, discussion, and review in several aspects.

Last but not least, I would like to thank my family for supporting me spiritually and financially throughout my master study and writing of this thesis.

University of Malaya

TABLE OF CONTENTS

Abstract	iii
Abstrak	iv
Acknowledgments.....	vi
Table of Contents.....	vii
List of Figures	x
List of Tables.....	xiii
List of Symbols and Abbreviations	xiv
CHAPTER1: INTRODUCTION.....	1
1.1 Overview.....	1
1.2 Motivations and Objectives.....	3
1.3 Scope and Organization.....	4
1.4 Contribution.....	5
CHAPTER 2: LITERATURE REVIEW.....	6
2.1 Introduction to Human's Heart.....	6
2.1.1 Cardiovascular systems.....	6
2.1.2 Autonomic nervous system.....	9
2.2 Introduction to Heart Rate Measurement Method.....	10
2.3 Photoplethysmography.....	11
2.4 Related Previous Work.....	14
2.4.1 Eulerian Video Magnification.....	14
2.4.2 Video Imaging for Targeted Subject.....	15

2.4.2.1	Blind Source Separation.....	15
2.4.2.2	Estimation of heart rate pulses from the video.....	17
2.4.3	Complex Hardware Systems.....	18
2.4.3.1	Using Thermal Imaging as Non-contact Heart Rate Measuring system.....	18
2.4.3.2	Using Direct Beam Laser Doppler Vibrometer as Non-contact Heart Rate Measuring system.....	20
2.4.3.3	Using Simultaneous Dual-Wavelength Photoplethysmography (PPG) as Non-contact Heart Rate Measuring system.....	21
2.5	Independent Component Analysis.....	22
2.6	Canonical Component Analysis.....	23
2.7	Color Spaces.....	25
2.7.1	RGB Component (Red, green and blue)	25
2.7.2	HSV (Hue, saturation, and value).....	26
2.7.3	Lab (Lightness, a and b).....	27
CHAPTER 3: SYSTEM DESIGN.....		28
3.1	Introduction.....	28
3.2	Pre-processing of Input Signal.....	29
3.3	Blind Source separation by using Canonical Component Analysis (CCABSS)	30
3.4	Rescaling and Bandpass Filter.....	31
3.5	Fast-Fourier Transform.....	34

CHAPTER 4: EXPERIMENTAL STUDY AND RESULTS.....	36
4.1 Introduction.....	36
4.2 Dynamic heart rate variation.....	36
4.2.1 Experiment Setup.....	36
4.2.2 First experiment: observed heart rates varying from low to high.....	37
4.2.3 Second experiment: observed heart rates varying from high to low.....	44
4.3 Distance between the subject and video camera.....	51
4.3.1 Varying distance with fixed video duration.....	51
4.3.2 Fixed distance with varying video duration.....	54
CHAPTER 5: CONCLUSION.....	57
References.....	60
List of Publications and Papers Presented	64
Appendix	65

LIST OF FIGURES

Figure 2.1: Chambers of the heart.....	6
Figure 2.2: Circulatory System.....	8
Figure 2.3: The heart conduction system.....	9
Figure 2.4: Autonomic Nervous system (ANS).....	10
Figure 2.5: ECG Setup.....	11
Figure 2.6: Layers of the normal human skin.....	12
Figure 2.7: ECG signal compared to the AC component of a PPG signal.....	13
Figure 2.8: Light-emitting diode (LED) and photodetector (PD) placement for transmission- and reflectance-mode photoplethysmography (PPG).....	13
Figure 2.9: PPG reflection and transmission modes.....	14
Figure 2.10: Process of Eulerian Video Magnification Methods.....	15
Figure 2.11: Experiment Setup for Blind Source Separation (ICA).....	16
Figure 2.12(a): Raw Thermal Image.....	19
Figure 2.12(b): Tracked Image.....	19
Figure 2.12(c): White line in the subject's neck represents the tracked blood vessel...	20
Figure 2.13: Experiment Setup for using Direct Beam Laser Doppler Vibrometer as Non-contact Heart Rate Measuring system.....	20
Figure 2.14: Experiment setup by using Simultaneous Dual-Wavelength Photoplethysmography (PPG) as Non-contact Heart Rate Measuring system.....	22
Figure 2.15: Visualization of RGB Colour Spaces.....	26
Figure 2.16: Visualization of HSV Colour Spaces.....	26
Figure 2.17: Visualization of Lab Colour Spaces.....	27
Figure 3.1: Workflow to extract the heart rate reading from video sequences.....	29
Figure 3.2: ROI Selection.....	30
Figure 3.3: Rescaling Process for RGB Component.....	32-33
Figure 3.4: BandPass Filter for RGB Component.....	33-34
Figure 3.5: Obtained signal in the frequency domain.....	35

Figure 4.1: Average RMSE values for all eight subjects in first experiment with duration vary from 3s to 7s.....	38
Figure 4.2(a): Comparison between actual heart rate readings and computer heart rate readings in the first experiment for all eight subjects by using CCA (4.5s).....	40
Figure 4.2(b): Comparison between actual heart rate readings and computer heart rate readings in the first experiment for all eight subjects by using ICA (4.5s).....	40
Figure 4.2(c): Comparison between actual heart rate readings and computer heart rate readings in the first experiment for all eight subjects by using CCA(5s).....	41
Figure 4.2(d): Comparison between actual heart rate readings and computer heart rate readings in the first experiment for all eight subjects by using ICA (5s).....	41
Figure 4.2(e): Comparison between actual heart rate readings and computer heart rate readings in the first experiment for all eight subjects by using CCA (6s).....	42
Figure 4.2(f): Comparison between actual heart rate readings and computer heart rate readings in the first experiment for all eight subjects by using ICA (6s).....	42
Figure 4.2(g): Comparison between actual heart rate readings and computer heart rate readings in the first experiment for all eight subjects by using CCA (7s).....	43
Figure 4.2(h): Comparison between actual heart rate readings and computer heart rate readings in the first experiment for all eight subjects by using ICA (7s).....	44
Figure 4.3: Average RMSE values for all eight subjects in second experiment with duration vary from 3s to 7s	45
Figure 4.4(a): Comparison between actual heart rate readings and computer heart rate readings in the second experiment for all eight subjects by using CCA (4.5s).....	46
Figure 4.4(b): Comparison between actual heart rate readings and computer heart rate readings in the second experiment for all eight subjects by using ICA (4.5s).....	47
Figure 4.4(c): Comparison between actual heart rate readings and computer heart rate readings in the second experiment for all eight subjects by using CCA (5s).....	48
Figure 4.4(d): Comparison between actual heart rate readings and computer heart rate readings in the second experiment for all eight subjects by using ICA (5s).....	48
Figure 4.4(e): Comparison between actual heart rate readings and computer heart rate readings in the second experiment for all eight subjects by using CCA (6s).....	49
Figure 4.4(f): Comparison between actual heart rate readings and computer heart rate readings in the second experiment for all eight subjects by using ICA (6s).....	49
Figure 4.4(g): Comparison between actual heart rate readings and computer heart rate readings in the second experiment for all eight subjects by using CCA (7s).....	50

Figure 4.4(h): Comparison between actual heart rate readings and computer heart rate readings in the second experiment for all eight subjects by using ICA (7s)..... 50

Figure 4.5: Box-Plot Graph of error values for all subjects with a duration time of 5 Seconds..... 53

Figure 4.6: Box-Plot Graph of error values for all subjects with a duration time of 8 Seconds..... 54

Figure 4.7: Box-Plot Graph of error values for all subjects with a distance of 50cm ...55

Figure 4.8: Box-Plot Graph of error values for all subjects with a distance of 100cm ..56

University of Malaya

LIST OF TABLES

Table 3.1: Example of the covariance matrices of input X and Y.....	31
Table 4.1: Summary of heart rate readings results in the first experiment (5s)	39
Table 4.2: Summary of heart rate readings results in the first experiment (7s)	39
Table 4.4: Summary of heart rate readings results in the second experiment (5s)	45
Table 4.4: Summary of heart rate readings results in the second experiment (7s)	45
Table 4.5: RMSE values for a distance varying from 30cm to 200cm with 5-seconds duration.....	52
Table 4.6: RMSE values for distance varying from 30cm to 200cm with 8-seconds duration.....	53
Table 4.7: RMSE values for varying duration time at distance of 50cm.....	55
Table 4.8: RMSE values for varying duration time at distance of 100cm.....	55

LIST OF SYMBOLS AND ANNREVIATIONS

ANS	:	Autonomic Nervous System
AVN	:	Atrioventricular Node
BPM	:	Beat per Minute
BSS	:	Blind Source Separation
BVP	:	Blood Volume Pulse
CCA	:	Canonical Component Analysis
CCABSS	:	Blind Source Separation by using Canonical Component Analysis
ECG	:	Electrocardiography
HSV	:	Hue, Saturation, and Value
ICA	:	Independent Component Analysis
LED	:	Light Emitting Diodes
MWIR	:	Mid-Wave Infrared
PPG	:	Photoplethysmography
RGB	:	Red, Green and Blue
RMSE	:	Root Mean Square Error
ROI	:	Region of Interest
SA	:	Sinoatrial Node
VCSEL	:	Vertical Cavity Surface Emitting Laser

CHAPTER 1: INTRODUCTION

1.1 Overview

One of the parameters that are widely used both in sports and healthcare is the human heart rate. It is measured as the number of heart beats per minute (BPM). Currently, the Electrocardiography (ECG) machine, which is a contact based method, is the most common method to measure human heart rate. In this method, the human heart rate is obtained from the analysis of the electrical activity of the heart through the attached electrodes around the wrist and chest area. However, the ECG machine might not be suitable for those patients with sensitive skins (Teichmann et al., 2012; Yu et al., 2015). Given the significance of heart rate measurements and advancements in technology, there is a renewed interest to look at alternative and low-cost methods.

Garbey et al. introduced a new approach for human cardiac pulse measurement based on thermal signal analysis of the major blood vessels near the skin surface (Garbey et al., 2007). The modulation of the temperature measured from these blood vessels is caused by the variations in blood flow. In the same year, Pavlidis et al. measured the human heart rate and breath rate through bio-heat modeling of facial imagery using a thermal camera (Pavlidis et al., 2007). The cardiac pulse detection at the forehead proposed by Gatto was extracted from the video infrared thermography (Gatto, 2009). This approach is based on the principle that the variations of blood flow during the cardiac cycle will cause the fluctuation of thermal energy released by the body tissue.

Takano and Ohta developed a system to measure the human heart rate and respiratory rate based on the images from the Charge-Coupled Device camera (Takano & Ohta, 2007). The variations of the average brightness in the region of interest within the subject's skin were recorded. These data were processed through a sequence of

operations which involves interpolation, low pass filter, and auto-regressive spectral analysis to obtain the heart rate and the respiratory rate. In the following year, Verkruysse et al. measured human respiration and heart rates through remote sensing of plethysmographic signals under ambient light using a digital camera (Verkruysse et al., 2008).

Jonathan and Leahy utilized the camera on the smartphone to capture a series of video frames of a human index finger (Jonathan & Leahy, 2010). The reflections of plethysmographic signals obtained from these video frames were used to compute the human heart rate. The engineering model created by Shi et al. was used for cardiac monitoring through reflection photoplethysmography (Shi et al., 2010). This non-contact model is made up of a light source that consists of a Vertical Cavity Surface Emitting Laser (VCSEL) and a photo-detector that consists of a high-speed silicon PiN photodiode.

Photoplethysmography (PPG) has been explored by researchers to measure the human heart rate. In the early part of using PPG to measure heart rate, researchers have been investigating the relationship between the blood volume pulses and the light in reflection PPG (Hertzman, 1938; Weinman et al., 1977). Due to the way the heart operates during each cardiac cycle, the intensity of reflectance changes accordingly. Based on this relationship, Kamshilin et al. presented a novel methodology for the formation of PPG images from video recordings of a living body in the reflection geometry (Kamshilin et al., 2011). The heart rate can then be obtained from the PPG signals captured in the video.

Based on the color variations of the face due to blood circulation, Poh et al. introduced a robust image analysis to obtain the heart rate from the facial image in the video sequences (Poh et al., 2010, 2011). In overcoming motion artifacts, which are not dealt properly will render inaccurate heart rate reading they applied blind source

separation (BSS) on the color channels to obtain the human heart rate from facial images of the video. Pursche et al. modified this technique by transforming the BSS source signals (the heart rate signals) into the frequency domain to obtain the heart rate (Pursche et al.,2012). In their work, the face was divided into three parts, and they found using the center of the face region gave better results when compared to the other two areas.

A simplified mathematical model to obtain the BPM signals from images of human skin is introduced by Xu et al. (Xu et al., 2014). Their model was based on pigment concentration in the human skin. Meanwhile, Kumar et al. proposed a model, known as DistancePPG, which used a weighted average assigned to different regions of the face. Their method improves the signal-to-noise ratio of the camera-based PPG signal thereby significantly improved the accuracy of heart (Kumar et al., 2015).

Using the Microsoft Kinect Visual and Depth Sensors, Procházka et al. developed a non-contact heart rate measurement system (Procházka et al., 2016). In this study, video frames of facial features and thorax movements are recorded by Microsoft Kinect image, depth, and infrared sensors to estimate the heart rate. Hamedani et al. introduce a non-contact measurement of heart rate using thermal imaging (Hamedani et al., 2016). The thermal variations caused by blood circulation were extracted from recorded thermal imaging from three different areas of the face. The heart rate was then obtained using two methods including zero crossing and Fast Fourier Transform.

1.2 Motivations and Objectives

In this thesis, a new and novel method to measure heart rate from a video sequence is introduced. Since the heart rate varies insignificantly within a second with the existence of artifacts and noises, it is assumed that the heart rate signals are strongly correlated to each other and the random artifacts and noises appearing in two video frames are not correlated to each other. By examining the most correlated signal within these two

video frames using Canonical Component Analysis (CCA), the heart rate can be estimated.

On the other hand, an important consideration in estimating the instantaneous heart rate is to use a limited number of video frames or video duration. If the video duration is too long, the model may not report the accuracy for large heart rate variations. Therefore, the number of video frames should be taken into account when designing the heart rate estimation model.

The objectives of this research are as follow:

- 1) To estimate human heart rates from video sequences by using CCA with a short duration.
- 2) To compare the results of the proposed method with an existing methods using Independent Component Analysis (ICA).
- 3) To estimate the accuracy of human heart rates from video sequences by varying the distance between the subject and video camera.
- 4) To estimate the accuracy of human heart rates by varying video duration but with fixed distance.

1.3 Scope and Organization

This thesis contains chapters describing the research findings and experimental studies about the dynamic heart rate estimation using CCA from video sequences. The following is the summary of the content of the chapters in this thesis.

- i. **Chapter 2: Literature Review.** This chapter presents the information about the human's heart, the cardiovascular system, autonomic nervous system, heart rate measurement method, photoplethysmography, previous related work, color spaces, and also the canonical component analysis.

- ii. **Chapter 3: System Design.** This chapter discusses the design of the system to measure the human's heart rate reading through videos sequences. Including the pre-processing of the input signal, region of interest, application of CCA, rescaling system, bandpass filter, and fast fourier transform.
- iii. **Chapter 4: Experiment Study and result.** This chapter discusses the experiment setup and results of the experiment. There is two categories of experiments were conducted in this thesis. For the first category, it involved dynamic heart rate of the subjects where the heart rate of the subjects will increasing or decreasing but fixed distance between camera and subjects. For the second category, the subjects' heart rate is stationary, but the distance of camera and subjects will vary. The results of the experiments also will be presented in this chapter.
- iv. **Chapter 5: Conclusion.** This chapter concludes the research works presented in the thesis. It summarizes the contents of the thesis.

1.4 Contribution

The contribution of this thesis is that it proposes a method to estimate the instantaneous heart. The proposed method can estimate heart rates that vary rapidly.

CHAPTER 2: LITERATURE REVIEW

2.1 Introduction to Human's Heart

The information about the human's heart will discuss in this chapter. First, we discuss the cardiovascular system, then the Autonomic Nervous system (ANS) of the human body.

2.1.1 Cardiovascular systems

The cardiovascular system consists of the heart, blood vessels and the approximately 5 liters of blood is the organ system that to transport the oxygen and nutrients such as electrolytes, amino acids, enzymes and hormones to human's body. At the same time, the cardiovascular system also removes the waste products and carbon dioxide through the lungs. Another function of the cardiovascular system is to regulate the body temperature, fluid pH, and water content of cells. All of these processes can be summarized as homeostasis, a process which maintains a condition of a dynamic balance or equilibrium within its internal environment, even when faced with external changes.

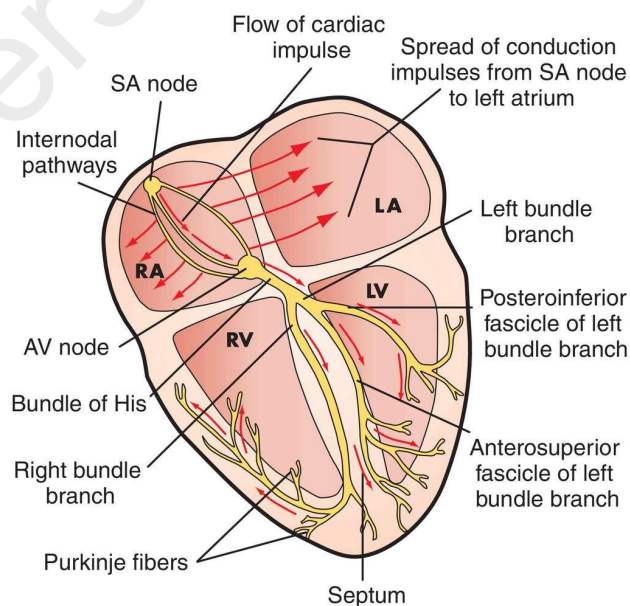


Figure 2.1: Chambers of the heart

(Mosby's Medical Dictionary (2009))

Refers to figure 2.1, there are four chambers of the heart which is the right atrium, left atrium, right ventricle, and left ventricle. The atria are the receiving chambers for blood. Therefore they are connected to the veins that carry blood to the heart. The ventricles are the large and stronger pumping chambers. Therefore, they are connected to the arteries that send the blood out of the heart. The “left heart” consist of the left atrium and left ventricle. The left ventricle is the largest and strongest chamber in the human heart. For the “right heart,” it consists of the right atrium and right ventricle. There is a wall of muscle called “Septum” to separate the two sides of the heart.

Refers to figure 2.2, there are two pathways called the pulmonary and systemic circulation are used for the blood transport in human’s body. In the pulmonary circulation, deoxygenated blood leaves the right ventricle of the heart via the pulmonary artery and travels to the lungs, then returns as oxygenated blood to the left atrium of the heart via the pulmonary vein. Instead, in the systemic circulation, oxygenated blood leaves the body via the left ventricle to the aorta and from there enters the arteries and capillaries where it supplies the body’s tissues with oxygen. Deoxygenated blood returns via veins to the vena cava, re-entering the heart’s right atrium where the systemic circulation ends.

From a mechanical point of view, the heart is considered as a pump, because it pumps blood through the entire circulation, to meet the requirements of all the cells of the body. The heart forces blood out of its chambers and relaxes to allow the next quantity of blood to enter. The contractions are named to systole and the relaxation diastole. Blood flows from an area of high pressure to an area of lower pressure. The myocardium is controlled by the electric activity of the heart that controls the timing of the heartbeat and the heart rhythm which is the synchronized pumping action of the heart chambers.

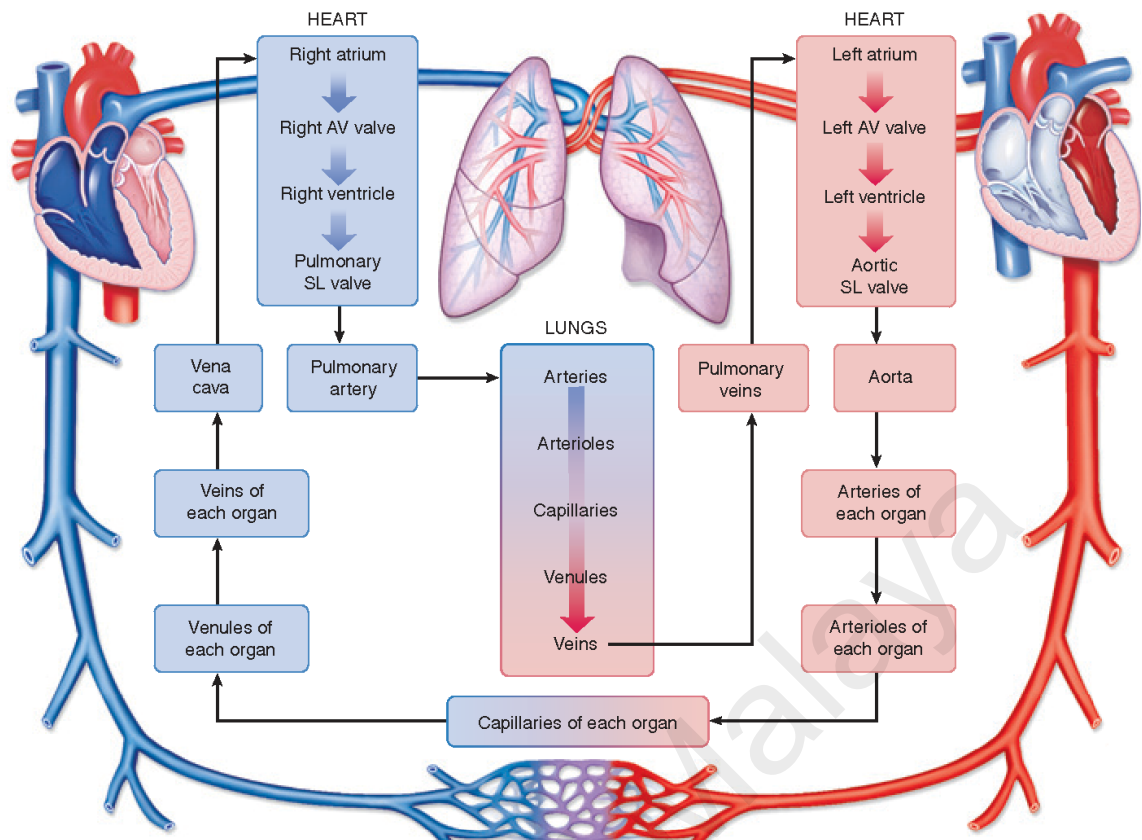


Figure 2.2: Circulatory System(Wilson(2012))

The heart conduction system consists of the sinoatrial node (SA), the intermodal pathways, the atrioventricular node (AVN), atrioventricular bundle and its branches and the Purkinje fibers. A complete heartbeat is conducted when an electrical impulse is generated from the SA node, then the signal will travel through the heart and triggering first two atria and then travels down to two ventricles. Details of the heart conduction system can refer to figure 2.3.

The heartbeat happens as follows:

1. The SA node generates an electrical impulse.
2. The upper heart chambers (atria) contract.
3. The Atrioventricular node (AVN) transfer impulse to the ventricles
4. The lower heart chambers (ventricles) contract and pump.
5. Then the cycle repeats itself.

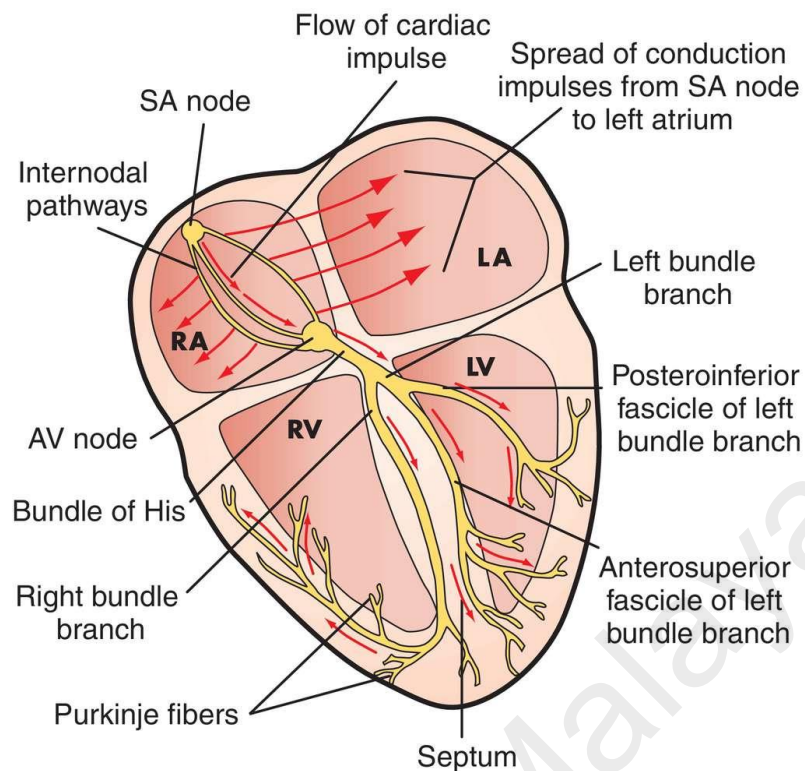


Figure 2.3: The heart conduction system(Baig (2019))

2.1.2 Autonomic nervous system

The Autonomic Nervous system (ANS) is the human's system that to regulate the activity of internal organs either is involuntarily or automatically. Example of the processes controlled by the autonomic nervous system is Blood Pressure, HR and Breathing, body temperature, digestion, metabolism, the balance of water and electrolytes, production of body fluids, urination, defecation, and sexual response. By referring to figure 2.4, there are two main branches of the autonomic nervous system, the Sympathetic and the Parasympathetic. Most of the times, the two branches have opposite effects on the same organ. For example, the sympathetic branch increases blood pressure, and the parasympathetic one decreases it. Overall the two branches work together to ensure that the body responds appropriately to different situations.

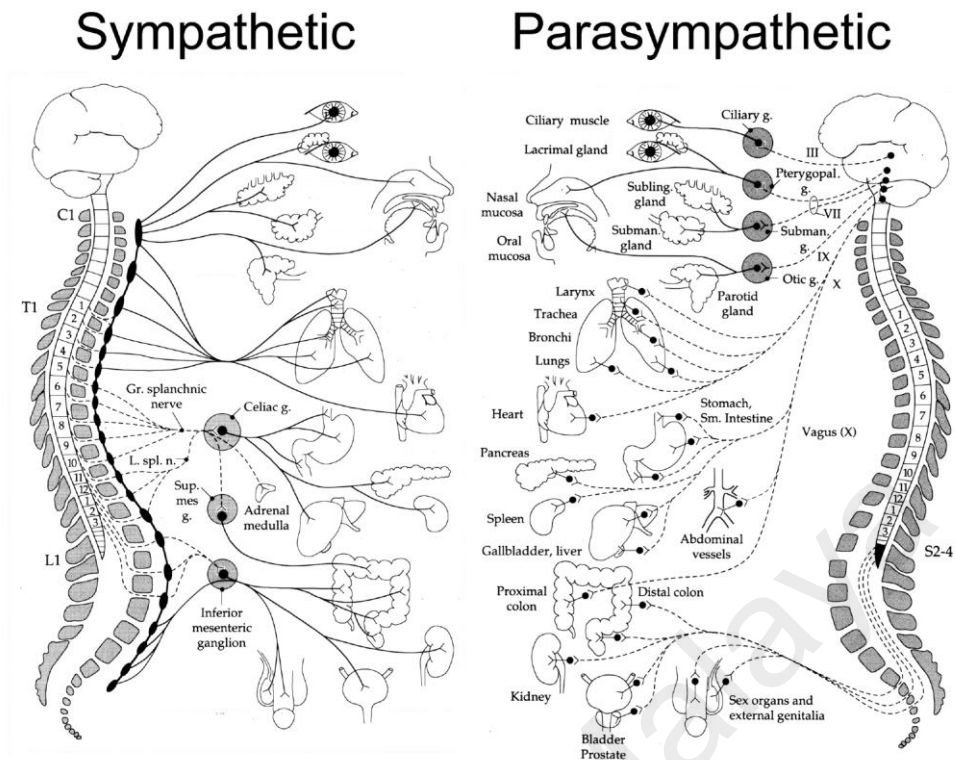


Figure 2.4: Autonomic Nervous system (ANS)(Karemaker (2017))

Among the main functions mentioned above, in this study only focus on the modulation of cardiac activity.

2.2 Introduction to Heart Rate Measurement Method

Heart rate is one of the most important physiological signals in the human body. It gives the most valuable meaning to the medical condition of the person. Heart rate is directly proportional to the absorb oxygen by the body. Therefore medical professionals will constantly check the heart rate reading of a patient. Usually, heart rate will express in beats per minute (BPM). On the other hand, heart rate also can use as an indicator of the fitness levels of athletes. Therefore athletes will monitor it to maximize the efficiency of their training.

Currently, due to the high accuracy and convenience, Electrocardiogram (ECG) is the most common method used by medical professions to check the heart rate of a patient. ECG will record the electrical activity of the heart, and this signal was related to heart contraction. Therefore it is equivalent to the heart rate. ECG records the signal by

attaching the several adhesive electrodes to the skin. Figure 2.5 shows the example of ECG system setup.

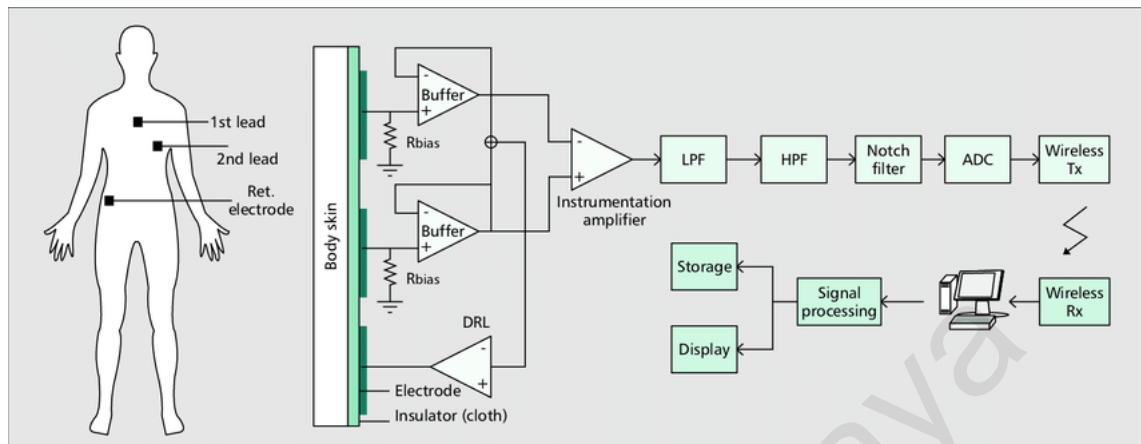


Figure 2.5: ECG Setup(Nemati et al. (2012))

Other than measuring the electrical activity of the heart, another method to measure heart rate is by measuring the Blood Volume Pulse which is the blood pumped by the heartbeat to the whole body through blood distribution network of the body, i.e., circulatory system. This method called Plethysmography. One of the most simple examples of plethysmography is pressing our fingers in a region of the body which affected by the flow of artery-like wrist or neck.

2.3 Photoplethysmography

Photoplethysmography (PPG) is the method to measure plethysmography signal by using optical means. Usually, it contained one light source and a photodetector to detect volume changes in human's skin tissue. Figure 2.6 shows the example of human skin and is formed by three main layers: Epidermis, Dermis, and Hypodermis. Currently, we still cannot completely understand how the light interacts with the skin tissue, i.e., how much light each component absorbs, scatters and reflects.

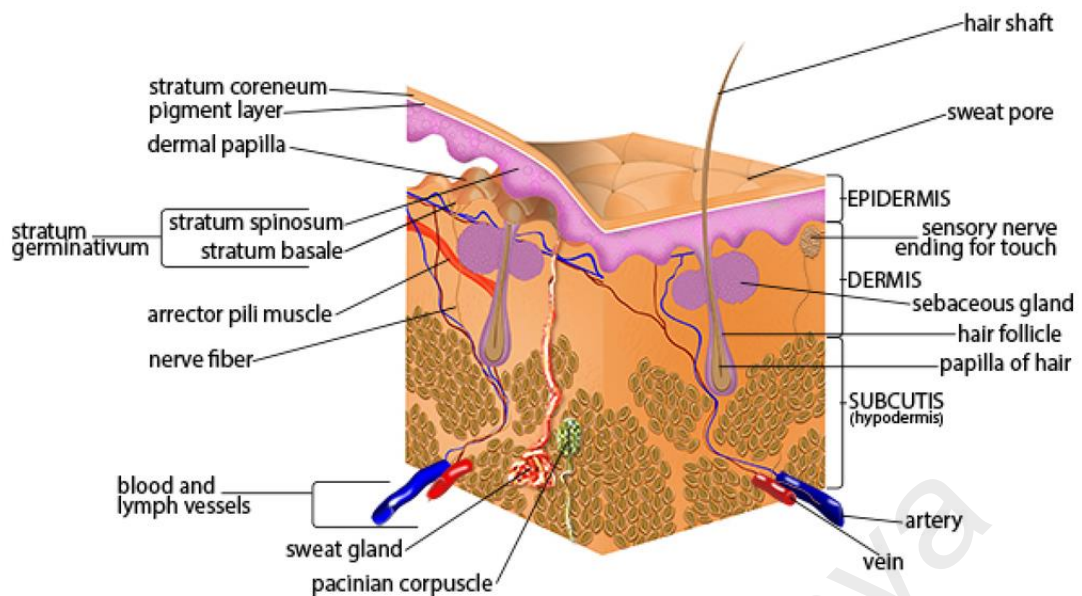


Figure 2.6: Layers of the normal human skin.(Vilhena & Ramalho (2016))

According to Allen, the blood will absorb more light compared to surrounding substances. Therefore, the PPG will record a waveform composed of two elements at different frequencies. The first component is the pulsatile component which reflects the synchronous variation of blood flow. It also called as “AC” component which directly related to the heart rate. The second component is the accounts for low-frequency phenomena, such as respiration, vasometric activity or thermoregulation and it is also called as “DC” Component. (Allen, 2007). A comparison between PPG and ECG is shown in figure 2.7, and we can notice that every heartbeat corresponds to a peak in AC component.



Figure 2.7: ECG signal compared to the AC component of a PPG signal (Allen, 2007)

Hertzman is the first establishment of PPG technique in the year 1938, and there are several issues encountered such as the use of regular light bulb that cannot provide stable light conditions. Mendelson and Ochs have established another PPG technique by examining the skin heating tested (Mendelson and Ochs, 1988). In the year 1989, Kamal et al. introduced the PPG technique using more stable light sources like light emitting diodes (LED) (Kamal et al., 1989). There are two PPG modes: transmission mode and reflection mode. In the transmission mode, the target sample like an earlobe, the fingertip is placed between the light source and the photodetector. In the reflection mode, both the light source and photodetector placed in the same side of the target sample. The example is shown in figure 2.8.

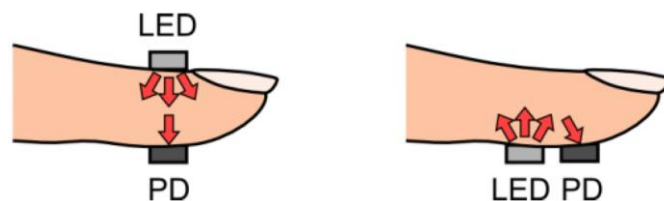


Figure 2.8: Light-emitting diode (LED) and photodetector (PD) placement for transmission- and reflectance-mode photoplethysmography (PPG) (Tamura et al. (2014))

A CMOS camera replaced the photodiode and maintained the light source in both PPG modes was introduced by Zheng et al., and they suspect that the DC

component only affected by breathing. (Zheng et al., 2008). Figure 2.9 shows the example of Zheng et al. study.

Although with a large constraint like no motion was allowed, and the skin region is manually selected, Verkrusse et al. were successful in performing PPG by using uniquely ambient light. They also found that under the ambient light, the green channel contains the strongest plethysmographic signal (Verkrusse et al., 2008). This was reported by previous studies which the green light is more easily absorbed by hemoglobin compared to red light (Van Kampen et al., 1965).

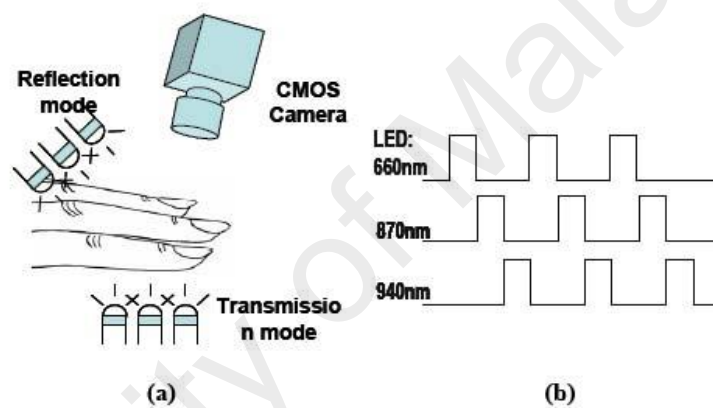


Figure 2.9: PPG reflection and transmission modes (Zheng et al. (2008)).

2.4 Related Previous Work

In this section, some of the previous researcher's work will be discussed.

2.4.1 Eulerian Video Magnification

According to Wu et al., Eulerian Video Magnification is a method that allows the user to identify the small color changes in videos which are hidden from the human eye (Wu et al., 2012). This method involves two main steps: spatial decomposing and temporal filtering. At first, the video sequence is decomposed into a different spatial frequency signal, and a temporal filter is applied to all bands. A predetermined factor α will then be applied to the filtered signal. Finally, the amplified signal is added to the original

signal and used to generate the desired signal. Frequencies within the range of 0.5-4 Hz are used to target the heart rate of 30 to 240 beats every 60 seconds. The value of amplifying factor used in this method was range from 0 to 100. Figure 2.10 shows the process of Eulerian Video Magnification methods.

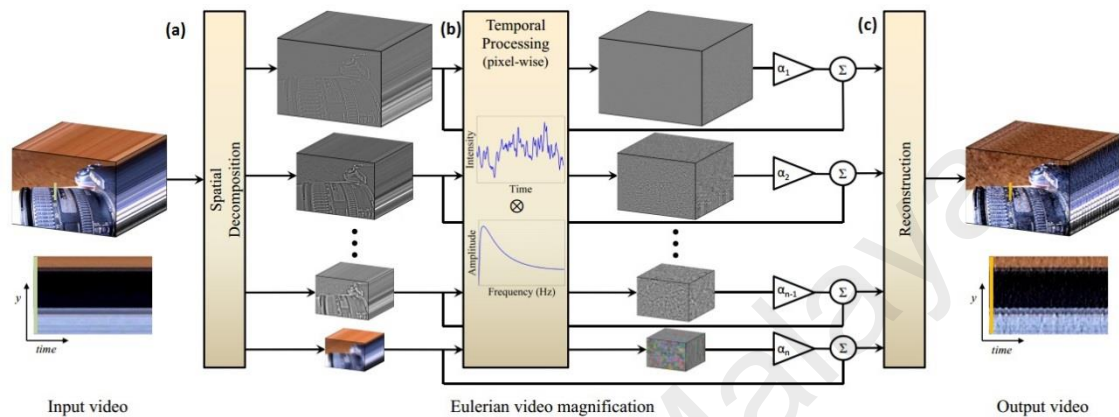


Figure 2.10: Process of Eulerian Video Magnification Methods (Wu et al. (2012))

2.4.2 Video Imaging for Targeted Subject

This section discusses two methods that use video images of the targeted subjects to obtain the heart rate. Both methods are explored deeply from two sides. First, explain the experiment setup. Second, discuss the core of the method that obtained the heart rate readings.

2.4.2.1 Blind Source Separation

Poh et al. proposed a non-contact method to measure cardiac pulse rate by using a simple (Poh et al., 2010, 2011). The subject will face to the webcam for 60-second video. Subjects are required to stay still with no motion. Heart rate reading of subjects will record simultaneously by using cardiovascular blood volume pulse sensor. The subject's face was tracked by using Open Computer Vision library which detects the face location using a box with x- and y- coordinates. The region of interest (ROI) is the center 60% of the width and full height of the tracked box. The ROI will then separate into three

channels: Red, Green, and Blue Channels. Next, the raw channel is formed and normalized, as per the equation below:

$$x'_i(t) = \frac{x_i(t) - \mu_i}{\sigma_i} \quad (2.1)$$

Where μ_i, σ_i are the mean and standard deviation of $x_i(t)$ for each i where $i = 1, 2, 3$.

After that, Independent Component Analysis (ICA) will then separate the normalized channels into independent source signals. After obtaining the independent source signals, Fast Fourier Transform was used to transform the independent source signal into frequency domain. A signal with the highest power on the spectrum was selected as the heartbeat rate. The operational frequency is 0.5 – 4 Hz or 30 – 240 beats per minute.

Figure 2.11 shows the experimental setup where the subject faces the laptop's built-in webcam.

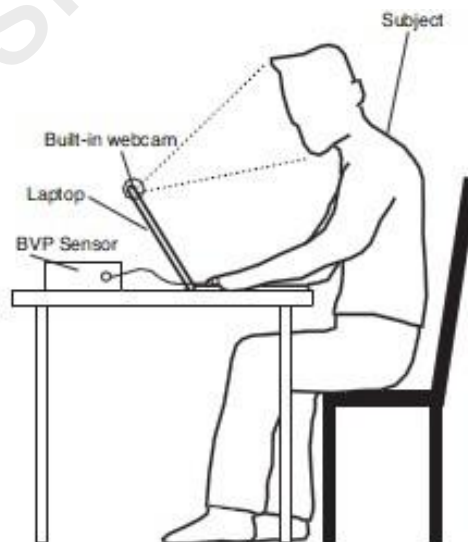


Figure 2.11: Experiment Setup for Blind Source Separation (ICA)
(Poh et al. (2010))

2.4.2.2 Estimation of heart rate pulses from the video

Xu et al. develop a similar experiment as Poh et al. but replace the ICA method with the new simplified mathematical model (Xu et al., 2014). According to Xu et al., the human heart rate can be predicted from video frames based on the absorbance of the lights by the skin.

The skin absorbance A at wavelength λ was defined as below:

$$A(\lambda) = v_m(\lambda)c_m + v_n(\lambda)c_n + A_o(\lambda), \quad (2.2)$$

Where c_m and c_n represent the pigment concentration for melanin and hemoglobin respectively, v is the product of pigment extinction coefficient and the mean path length of photons in the skin layer. A_o denotes the baseline skin absorbance and the residual pigment contribution.

According to Finlayson et Al. and Tsumura et Al.(Finlayson et al., 2004, Tsumura et al., 2003), the spectral function of a camera sensor can be considered as a delta function. Therefore the color components can be expressed in log space as

$$\log P_R = -\{v_m(R)c_m + v_n(R)c_n + A_o(R)\} + \log kE(R), \quad (2.3)$$

$$\log P_G = -\{v_m(G)c_m + v_n(G)c_n + A_o(G)\} + \log kE(G),$$

Where R and G were represented as the red and green channel of the image. k is a constant for the camera gain while E is the power of the transmitted light and incident light respectively.

Estimated heart rate signal can be obtained by the equation below:

$$y(n) = [\log \left(\frac{P_R^2 \cdot P_G^1}{P_R^1 \cdot P_G^2} \right), \dots, \log \left(\frac{P_R^n \cdot P_G^{n-1}}{P_R^{n-1} \cdot P_G^n} \right)] \quad (2.4)$$

After getting the estimated heart rate signal, the signal will then transform into the frequency domain by using Fast Fourier Transform. A signal with the highest power on the spectrum was selected as the heartbeat rate. The operational frequency is 0.5 – 4 Hz or 30 – 240 beats per minute.

2.4.3 Complex Hardware Systems

This section will present some complex hardware non-contact heart rate measuring system. There are two systems to be presented: thermal changes in the face and use a laser to measure pulse rate value invasively.

2.4.3.1 Using Thermal Imaging as Non-contact Heart Rate Measuring system

A novel non-contact heart rate measuring system by using a thermal camera was proposed by Garber et al. (Garber et al., 2007). This system assumes that the blood flow will produce high thermal changes on the blood vessels of the face. Therefore, the blood flow, pulse rate, and breathing rate can be captured by using a thermal camera. The thermal camera is connected to a computer. The heart rate measurements are computed by using design system in a computer.

In the experiment, the subject is required faces to a thermal camera which in this case is a Mid-Wave Infrared (MWIR) sensor, and the system will capture a period of record. MWIR sensor is sensitive to spectral range 3-5 μm .

Heart rate measurement will extract by following steps. First, localize the selection of the pixels concerning time. Figure 2.12 (a) shows the raw thermal images and figure 2.12(b) shows the tracked images. Next, the tracked frames are ready for blood vessel registration. Figure 2.12(c) shows a white line in the subject's neck which represents the tracked blood vessel. Fourier transform analysis applied on the obtained signals to extract its power spectrum. By using equation 2.5, the power spectra were

averaged to obtain the composite power spectrum, and the heart rate value is found by finding the dominant frequency.

$$P = \frac{1}{R_y} \sum_{y=0}^{R_y} P_y \quad (2.5)$$



Figure 2.12(a): Raw Thermal Image (Garber et al.(2007))



Figure 2.12(b): Tracked Image(Garber et al.(2007))



Figure 2.12(c): White line in the subject's neck represents the tracked blood vessel(Garber et al.(2007))

2.4.3.2 Using Direct Beam Laser Doppler Vibrometer as Non-contact Heart Rate Measuring system

Another non-contact heart rate measuring system by using laser Doppler vibrometer was developed by Scalise and Morbiducci (Scalise and Morbiducci, 2008). The idea of this method is by using an optical laser; the heart rate reading can be obtained by measuring the vibration of the main vessels on a subject's neck. Figure 2.13 shows the where the laser is directed at the subject's neck from a distance of 1.5 meters. The disadvantages of this method are the factors relating to the subject's positioning, and the equipment necessary is very difficult to achieve for an average user.

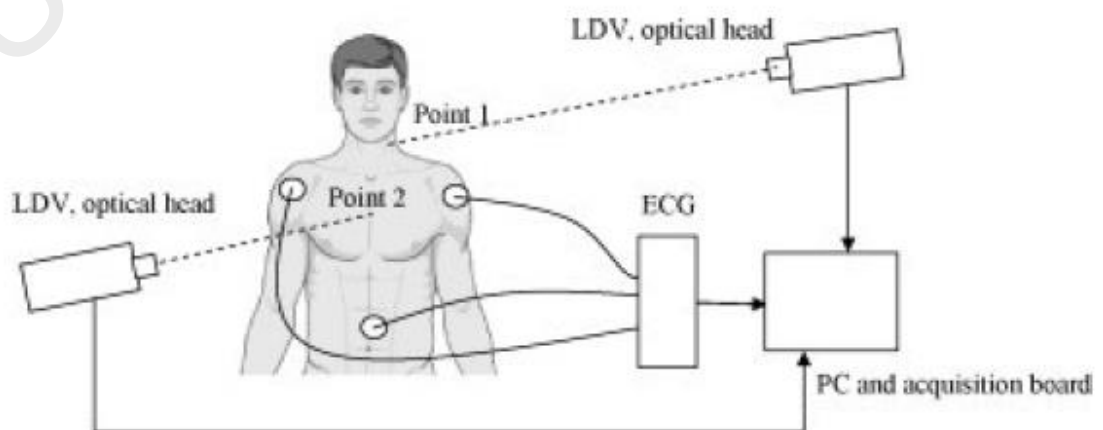


Figure 2.13: Experiment Setup for using Direct Beam Laser Doppler Vibrometer as Non-contact Heart Rate Measuring system (Scalise & Morbiducci(2008))

2.4.3.3 Using Simultaneous Dual-Wavelength Photoplethysmography (PPG) as Non-contact Heart Rate Measuring system

Humphreys et al. present a new contactless heart rate measurement system by using dual wavelength PPG signal (Humphreys et al., 2007). This method uses a camera that is capable of capturing two PPG signals at different wavelengths simultaneously. This experiment was done by using sophisticated equipment, and the obtained result was acquired with high accuracy.

The example of the camera was shown in figure 2.14. The system consists of a camera which equipped with a c-mount zoom lens and a 36 LED light source. The camera is zoomed manually to the targeted area, and a 20-second video was recorded. The distance between camera and subject's skin is 30cm, and the light source is located exactly beside the camera to illuminate the rest of the surface. Others part of the system like the computer connection and zoom lens was shown in the same figure. The idea of this method is to locate the presence of the reflected light source in the obtain video. This method can give the exactly equal results compared to result obtain from BVP sensor. There are some disadvantages for this method. First, difficult and costly setup process if compared to other method. Second, the allowed movement is very limited, and the distance must be located close to the subject. Therefore, it is not an ideal idea for a contactless heart rate system

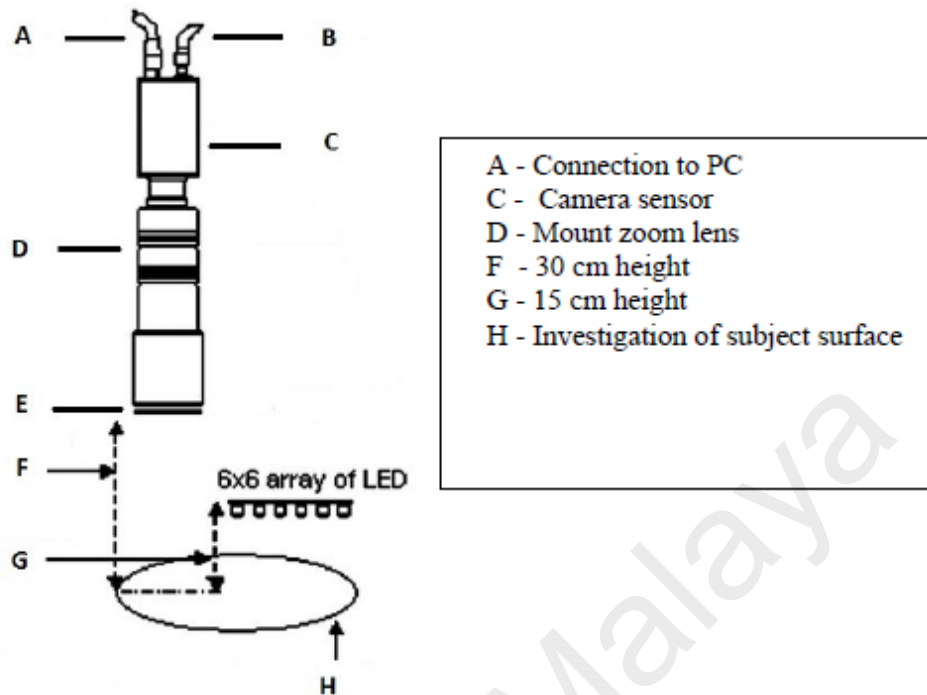


Figure 2.14: Experiment setup by using Simultaneous Dual-Wavelength Photoplethysmography (PPG) as Non-contact Heart Rate Measuring system (Humphreys et al. (2007))

2.5 Independent Component Analysis

Blind source separation (BSS) is used to recover the independent sources from a set of mixture source signals which obtain from sets of sensor observations. Source signals and how the signals were mixed were unknown Independent Component Analysis (ICA) is one of the methods to find the independent sources from unknown sources signals.

Assume that there are n linear mixtures (sensors) x_1, \dots, x_n of n independent components

$$X_j = a_{j1}s_1 + a_{j2}s_2 + \dots + a_{jn}s_n \text{ for all } j, \quad (2.6)$$

And each mixture x_j as well as the independent component s_k is a random variable, instead of a proper time signal. Let \mathbf{x} denotes as mixture unknown sources signals

x_1, \dots, x_n , \mathbf{s} denotes as independent source signals s_1, \dots, s_n , and \mathbf{A} denotes as unknown mixture matrix a_{ij} , then (2.6) can be written as

$$\mathbf{x} = \mathbf{A}\mathbf{s} \quad (2.7)$$

The (2.7) is described as independent component analysis. (Hyvärinen, A., & Oja, E., 2000). The unknown mixture matrix \mathbf{A} can be estimated and the independent components sources can be obtained by computing inverse of mixing matrix \mathbf{A} , which denoted as \mathbf{W} . Hence

$$\mathbf{s} = \mathbf{W}\mathbf{x} \quad (2.8)$$

There are two important criteria must be fulfilled when using ICA. First, the sources must be non-Gaussian distribution. Second, the sources are independent of each other.

For the video-based heart rate measurements and monitoring, the heart rate signal is the independent source signal of interest. The color components of the facial images captured by the video recorder, particular, red, green, and blue (RGB), vary in accordance to the heart rate variation since the changes in blood volume alter the light intensity reflected from facial tissue. Each of the RGB components is the sensor or mixture of the reflected plethysmographic signals and other sources (as well as the artifacts).

2.6 Canonical Component Analysis

Canonical Component Analysis (CCA) can be used as the solution to determine the relationship between two sets of variables. Suppose given a sample of instances $S = ((X_1, Y_1), \dots, (X_n, Y_n))$ of (x, y) . Let S_x denote as (X_1, \dots, X_n) , and S_y denote as (Y_1, \dots, Y_n) . Defines a new coordinate for x by choosing a direction W_x and projecting x onto that direction, and also same for y by choosing a direction W_y , therefore

$$S_{x, W_x} = ((W_x, X_1), \dots, (W_x, X_n)) \quad (2.9)$$

$$S_{y, W_y} = ((W_y, Y_1), \dots, (W_y, Y_n)) \quad (2.10)$$

CCA seeks a pair of linear transformations for variables x and y , such that maximum correlation (ρ) between x and y can be found when the variables are transformed. The correlation equation defined as:

$$\rho = \max_{W_x, W_y} \text{corr}(S_{x, W_x}, S_{y, W_y}) \quad (2.11)$$

Let denotes $\hat{E}[f(x, y)]$ as the empirical expectation of the function $f(x, y)$, where

$$\hat{E}[f(x, y)] = \frac{1}{m} \sum_{i=1}^m f(x_i, y_i), \quad (2.12)$$

We can rewrite correlation equation as

$$\begin{aligned} \rho &= \max_{W_x, W_y} \frac{\hat{E}[(W_x, x)(W_y, y)]}{\sqrt{\hat{E}[(W_x, x)^2] \hat{E}[(W_y, y)^2]}} \\ &= \max_{W_x, W_y} \frac{W'_x \hat{E}[xy'] W_y}{\sqrt{W'_x \hat{E}[xx'] W_x W'_y \hat{E}[yy'] W_y}} \end{aligned} \quad (2.13)$$

Let C denotes as covariance matrix of (x, y) where C is

$$C(x, y) = \hat{E} \begin{bmatrix} x \\ y \end{bmatrix} \begin{bmatrix} x \\ y \end{bmatrix}' = \begin{bmatrix} C_{xx} & C_{xy} \\ C_{yx} & C_{yy} \end{bmatrix}$$

Where C_{xx} and C_{yy} are within-sets covariance matrices and C_{xy} and C_{yx} are between-sets covariance matrices. Rewrite the correlation equation (2.13) as

$$\rho = \max_{W_x, W_y} \frac{W'_x C_{xy} W_y}{\sqrt{W'_x C_{xx} W_x W'_y C_{yy} W_y}} \quad (2.14)$$

The maximum value of correlation (ρ) can be obtained by maximizing the numerator subject to

$$W'_x C_{xx} W_x = 1 \quad (2.15)$$

$$W'_y C_{yy} W_y = 1 \quad (2.16)$$

Apply Lagrange multipliers method, the corresponding equation as below

$$L(\lambda, W_x, W_y) = W'_x C_{xy} W_y - \frac{\lambda_x}{2} (W'_x C_{xx} W_x - 1) - \frac{\lambda_y}{2} (W'_y C_{yy} W_y - 1) \quad (2.17)$$

Taking derivatives concerning W_x and W_y ,

$$\frac{\partial L}{\partial W_x} = C_{xy}W_y - \lambda_x C_{xx}W_x = 0 \quad (2.18)$$

$$\frac{\partial L}{\partial W_y} = C'_{xy}W_x - \lambda_y C_{yy}W_y = 0 \quad (2.19)$$

Multiply equation (2.18) with W'_x and equation (2.19) with W'_y , substitute by equation (2.15) and (2.16)

$$\lambda_x = W'_x C_{xy}W_y \quad (2.20)$$

$$\lambda_y = W'_y C'_{xy}W_x = W_y C_{yx}W'_x = \lambda_x \quad (2.21)$$

Since $\lambda_y = \lambda_x = \lambda$, now the equation (2.18) can rewrite as below

$$C'_{xy}W_x - \lambda C_{yy}W_y = 0$$

$$W_y = \frac{C_{yx}W_x C_{yy}^{-1}}{\lambda} \quad (2.22)$$

Replace equation (2.22) into (2.20); we can get

$$C_{xx}^{-1} C_{yy}^{-1} C_{xy} C_{yx} W_x = \lambda^2 W_x \quad (2.23)$$

Rewrite the equation (2.19) and substitute into equation (2.21), we can get W_y as

$$C_{xx}^{-1} C_{yy}^{-1} C_{xy} C_{yx} W_y = \lambda^2 W_y \quad (2.24)$$

2.7 Color Spaces

Throughout the thesis, the system will perform with color spaces. Definition of a color space is a method to describe colors by numbers. These numbers are called a color component. The color spaces discussed in this section are the RGB component (red, green and blue), the HSV component (hue, saturation, and value) and the Lab component (lightness, a and b).

2.7.1 RGB Component (Red, green and blue)

The RGB component is the most commonly used for many applications. These components are presented as a mixture of red color, green color, and blue color. A number of 0 or 1 can represent each of the components. For example, the Red is represented by {1;0;0} where white is represented by {1;1;1}. Figure 2.15 shows the

visualization of RGB color space. According to Bowmaker and Dartnall. The RGB color is the primary colors that connected to the physiology of the human eye, which are the most common photoreceptor cells responds to wavelengths respectively. (Bowmaker, J. K., & Dartnall, H., 1980)

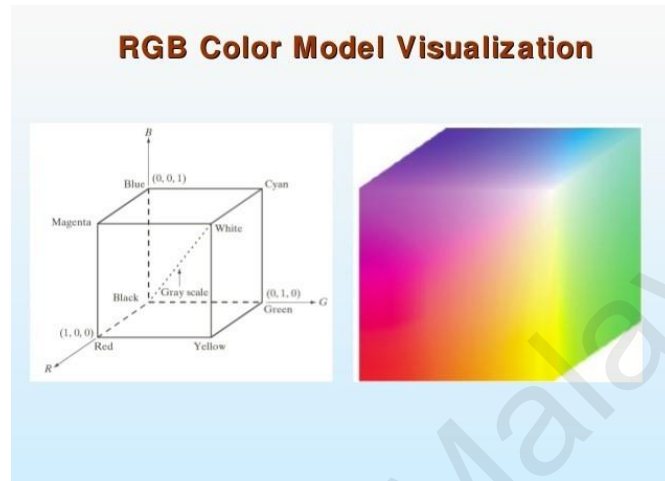


Figure 2.15: Visualization of RGB Colour Spaces
(Retrieved from <https://www.slideshare.net/lineking/10-color-image-processing-dip>)

2.7.2 HSV (Hue, saturation, and value)

HSV is a cylindrical-coordinate colour representation model Hue represents a pure color about the cylinder. Saturation represents the purity of color ranging from white a pure color. The value represents an illumination from black to a bright color. Figure 2.16 shows a visualization of HSV model. From figure 2.16, we can see that the red color being at 0 radians, green color at $\frac{2\pi}{3}$ radians and blue colour at $\frac{4\pi}{3}$ radians.

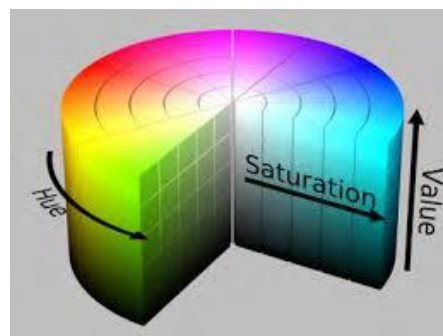


Figure 2.16: Visualization of HSV Colour Spaces (Retrieved from https://commons.wikimedia.org/wiki/File:HSV_color_solid_cylinder.png)

2.7.3 Lab (Lightness, a and b)

In Lab colorspace model, it consists of Lightness component L and two color component named a and b . Referring to figure 2.17, lightness component L is the central axis where a is x-axis and b is z-axis. The main idea for this color space is that a color cannot be both red and green or both blue and yellow. Therefore the positive value of a represents the amounts of red and negative value represents the amount of green. The same idea applied to component b which positive value of b represents the amounts of yellow and negative value of b represents the amount of blue.

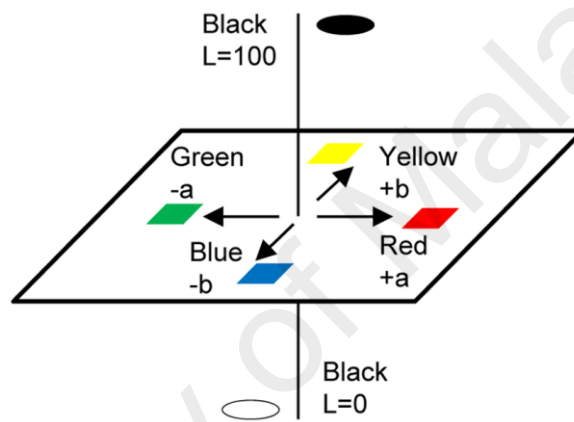


Figure 2.17: Visualization of Lab Colour Spaces (Liu et al. (2014))

CHAPTER 3: SYSTEM DESIGN

3.1 Introduction

In this section, the proposed method to estimate heart rate measurement is discussed. Let X and Y denote the data obtained from computing the facial image for five seconds, where Y begins one-second later. In this study, the camera records 50 frames per second. Hence X and Y can be expressed as

$$X = [\mu(t1), \dots, \mu(t250)]$$

$$Y = [\mu(t51), \dots, \mu(t300)]$$

CCA will determine the relationship between X and Y by computing their correlation values (ρ). Since Y begins one second after X , the heart rate varies insignificantly within a second. It is assumed that these two 5-second video frames will contain the heart rate signals that are strongly correlated to each other and the random artifacts and noises appearing in both video frames are not correlated to each other. Therefore the desired heart rate will remain unchanged which can give maximum correlation values. The obtained eigenvalues and eigenvectors with maximum correlation values now can be used to find the desired sources by multiplying them with source X . Figure 3.1 shows the workflow to extract the heart rate reading from video sequences.

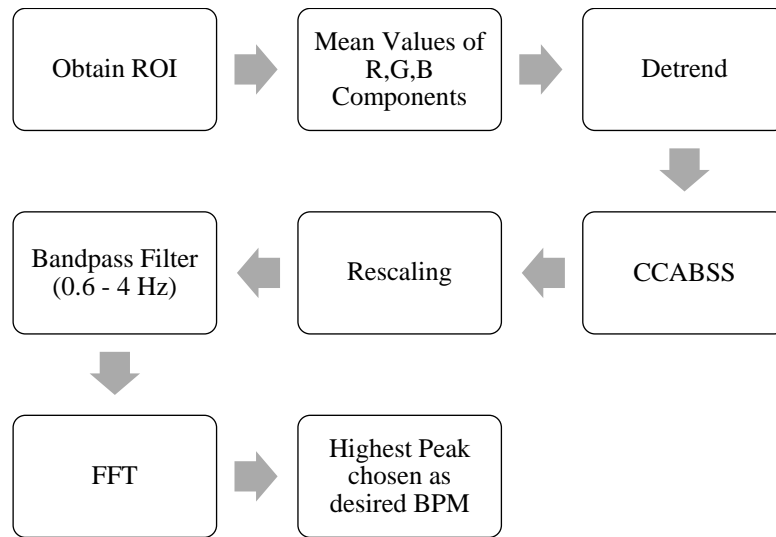


Figure 3.1: Workflow to extract the heart rate reading from video sequences

3.2 Pre-processing of Input Signal

The region of Interest (ROI) from subjects' face is defined for each frame of the images. There are two reasons to obtain the ROI for each frame of images. First is to increase the efficiency of processing time. Since fewer pixels were selected and be processed, thus the computation time also will decrease. The second reason is to reduce the noise in the extracted signal. There are only a few regions of human's face region able to prove the heart rate signal, an efficient selection of ROI will increase the accuracy of human heart rate extraction. According to Pursche et al. (2012), the region below eyes and above the upper lips of mouth will give the most accurate result. Figure 3.2 shows the example of ROI selection.



Figure 3.2: ROI Selection.

After obtaining the ROI, the mean value of pixel values in ROI region for red (R), green (G) and blue (B) components also computed separately,

μ_R : Mean value of all pixel values for R component

μ_G : Mean value of all pixel values for G component

μ_B : Mean value of all pixel values for B component

After getting the mean values of R, G and B component, all of these mean values were then detrended using an algorithm developed by Tarvainen et al.(2002).

3.3 Blind Source separation by using Canonical Component Analysis (CCABSS)

The obtained signal from the previous process will then pass into the CCABSS system developed by Borga, M., & Knutsson, H.(2001). The CCABSS will determine the eigenvalue and eigenvectors which provide the maximum correlation value of signal X and Y. The obtained eigenvalues and eigenvectors can be used to find the desired sources by multiplying them with signal X. Table 3.1 shows one example of the covariance matrices of input X and Y for R, G, B components.

Table 3.1: Example of the covariance matrices of input X and Y

Covariance Matrices, C		X			Y		
		R	G	B	R	G	B
X	R	0.929	0.613	0.555	0.085	0.128	0.112
	G	0.613	0.800	0.534	0.190	0.326	0.322
	B	0.555	0.534	0.825	0.140	0.164	0.156
Y	R	0.085	0.190	0.140	0.991	0.730	0.659
	G	0.128	0.326	0.164	0.730	1.001	0.730
	B	0.112	0.322	0.156	0.659	0.730	0.964

3.4 Rescaling and Bandpass Filter

A rescaling process to maximize the amplitude of the signals was applied to the obtained signal from CCABSS to minimize the effect of different amplitude. A 128-point Hamming window bandpass filter with a bandwidth of 0.6 to 4 Hz was then applied to the rescaled signal. Figure 3.3 shows the graphs before and after rescaling process for all R, G, B Component while figure 3.4 show the graphs for the signals before and after pass to the bandpass filter for all R, G, B Component.

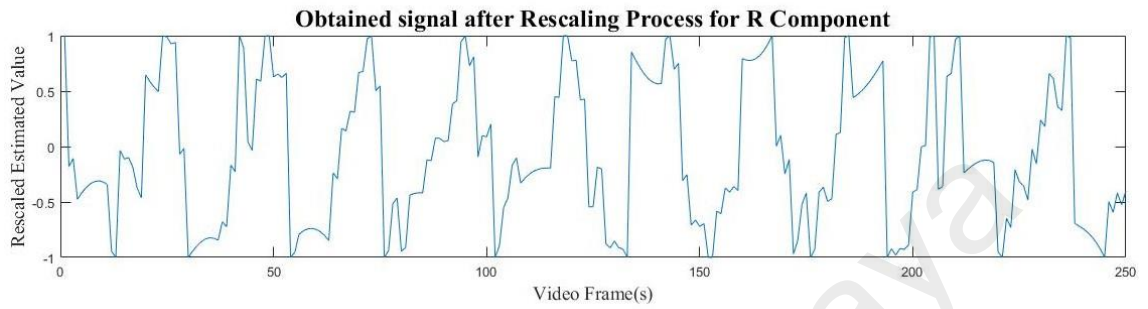
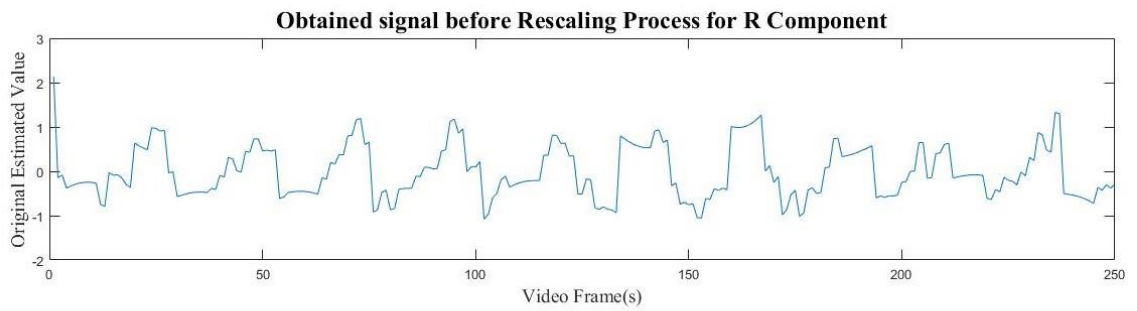


Figure 3.3(a): Rescaling Process for R Component

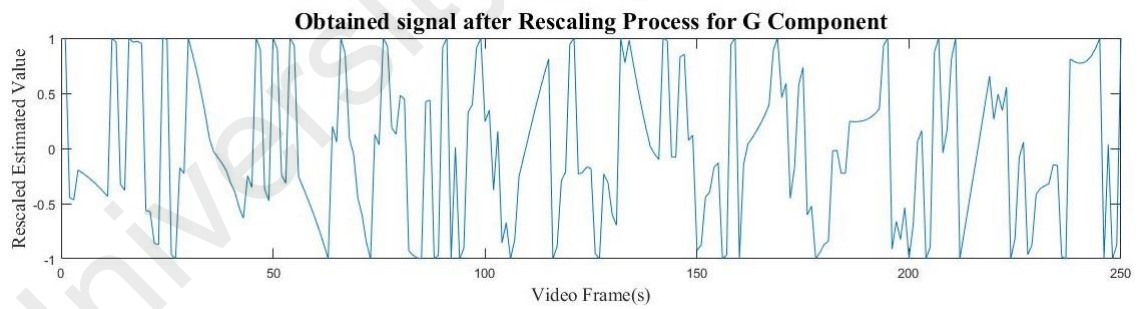
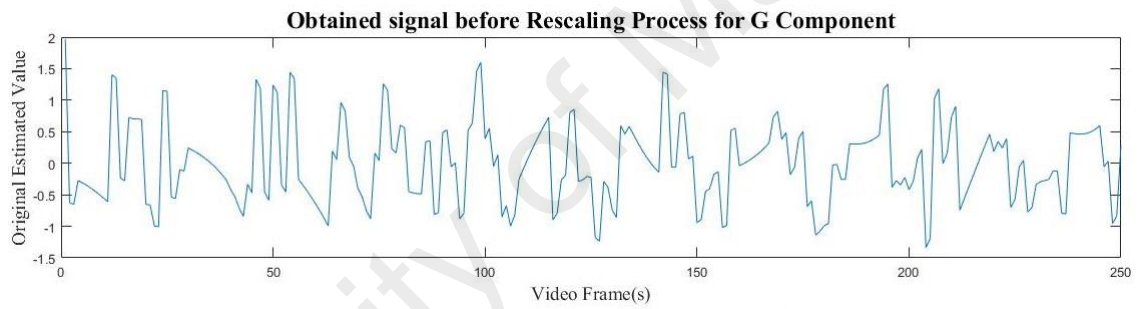


Figure 3.3(b): Rescaling Process for G Component

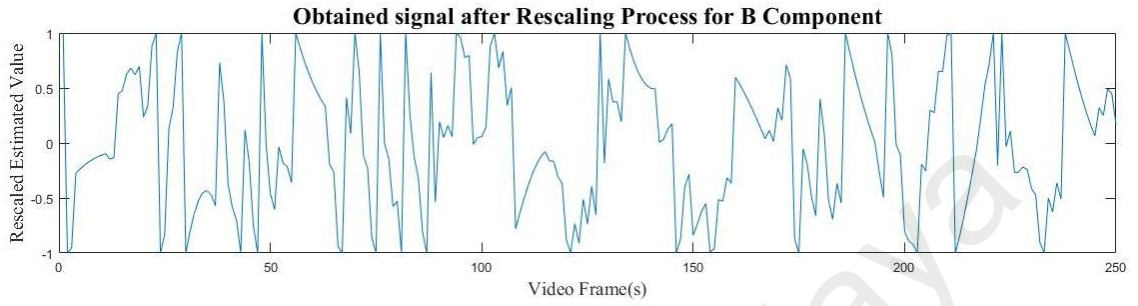
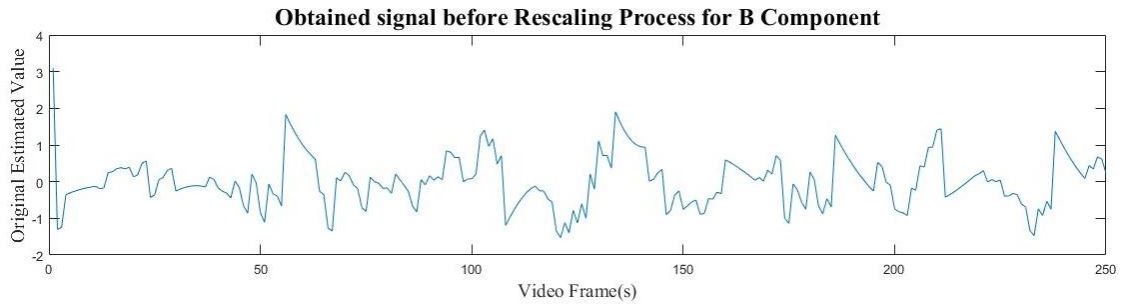


Figure 3.3(C): Rescaling Process for B Component

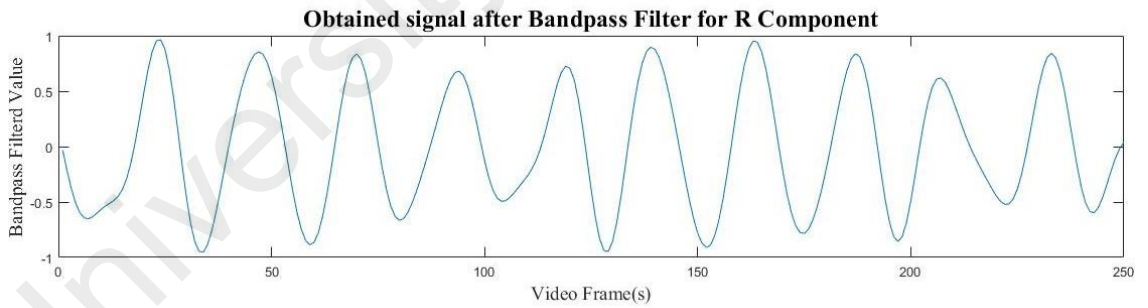
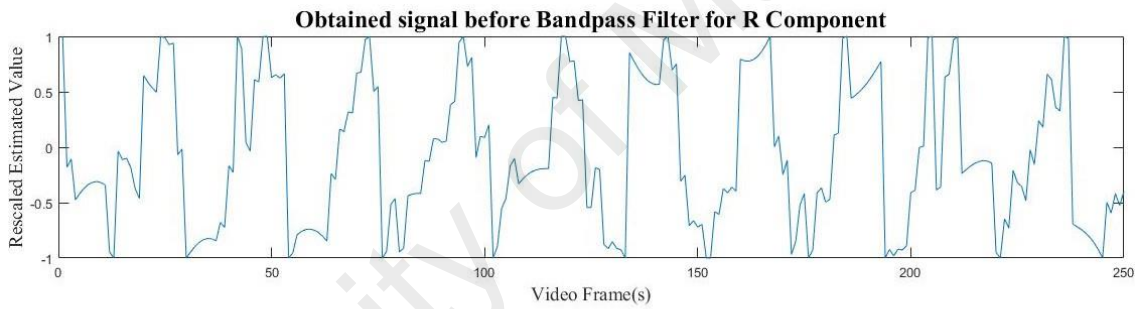


Figure 3.4(a): BandPass Filter for R Component

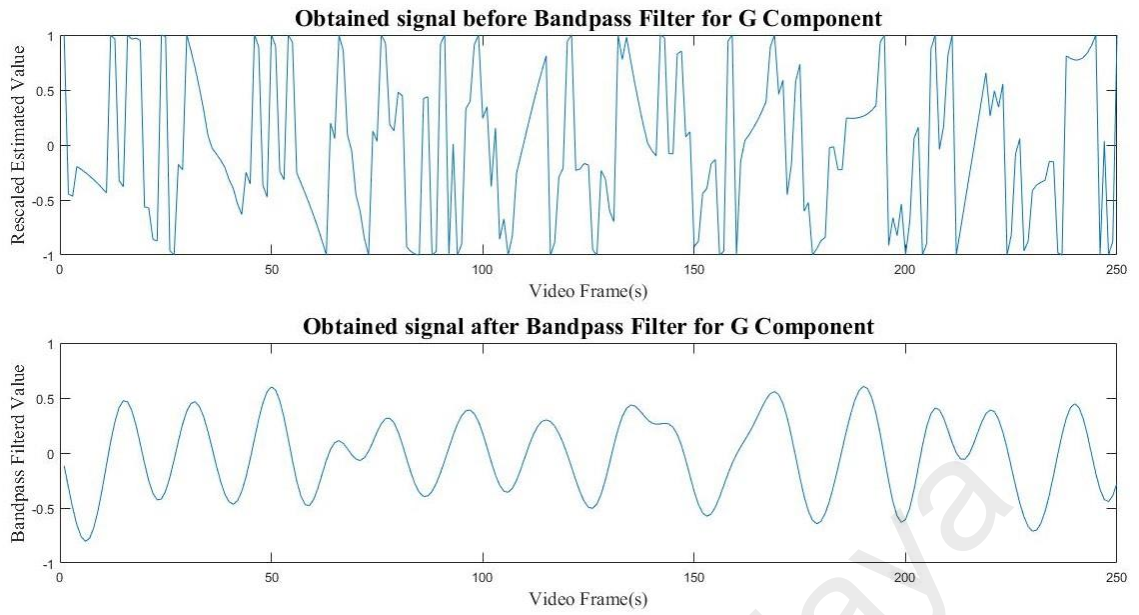


Figure 3.4(b): BandPass Filter for G Component

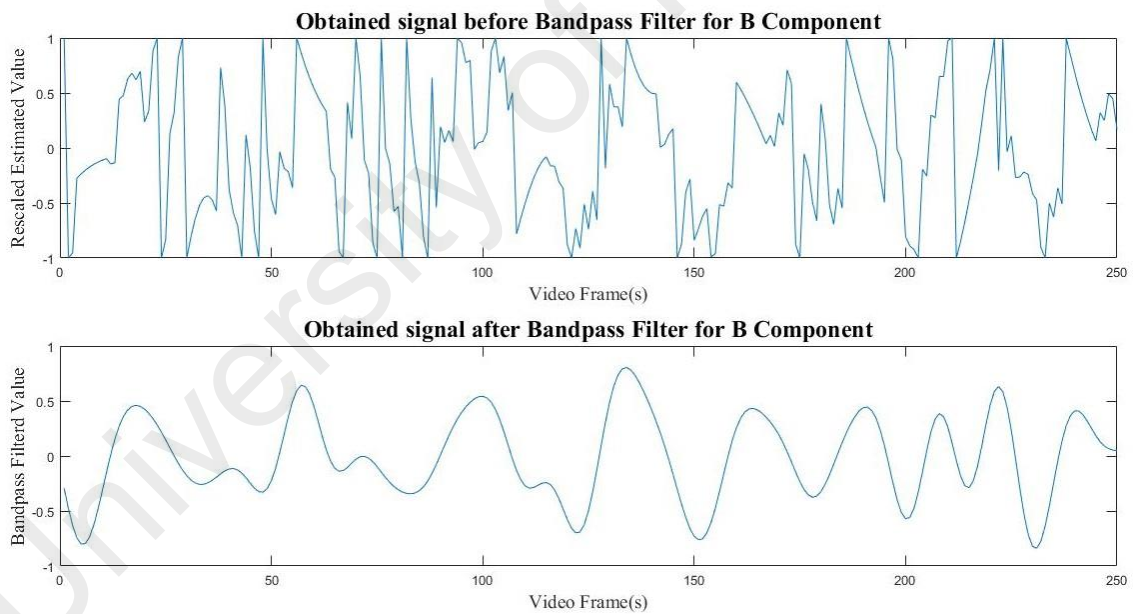


Figure 3.4(c): BandPass Filter for B Component

3.5 Fast-Fourier Transform

The obtained signal from previous bandpass filter process will then transform into the frequency domain by using fast-Fourier transform. The signal among R, G, B component that had the highest peak in the frequency domain was chosen as the BPM or heart rate value. Figure 3.5 shows the graph of the obtained signal in frequency

domain. From figure 3.5, we notice that R component gives the highest peak value (Y:0.7223) among three components. Therefore we can multiply the chose the x as our desired signal by multiply x with 60. In this case, x is 2.148 which give the value of 129 BPM.

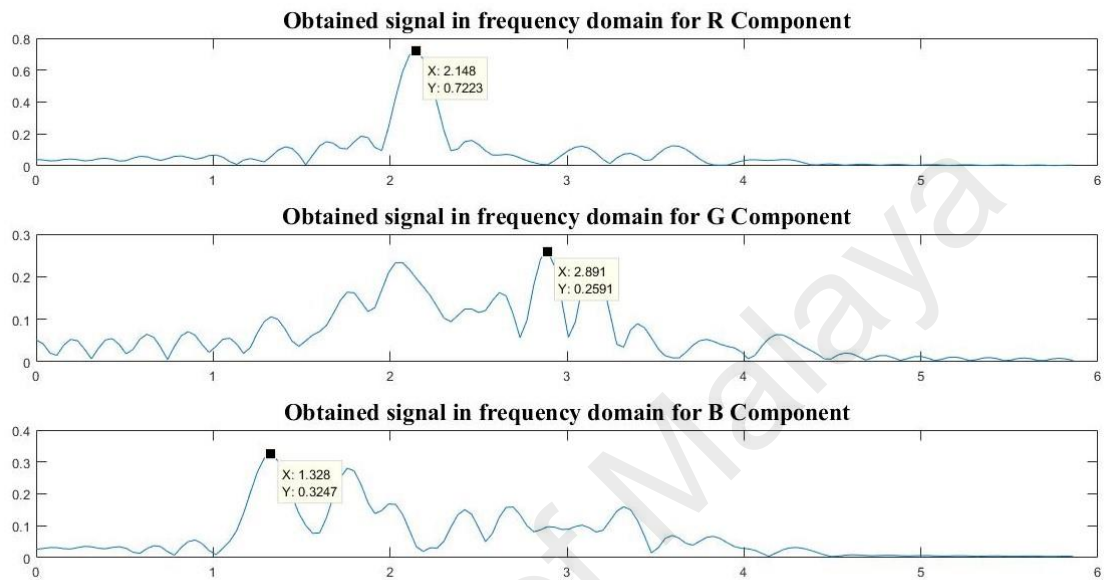


Figure 3.5: Obtained signal in the frequency domain

CHAPTER 4: EXPERIMENTAL STUDY AND RESULTS

4.1 Introduction

This section discusses the experimental setup and results. In the first part, two experiments related to dynamic heart rate variation for increasing and decreasing are discussed. On the other hand, the impact of varying the distance between the subject and the video camera and also fixing the distance but varying the video duration were conducted in second part of the experiment.

4.2 Dynamic heart rate variation

The experimental setup and the results of two experiments related to dynamic heart rate variation for increasing and decreasing are discussed. A total of eight subjects were involved in both experiments. Their heart rates varied from 75 to 150 BPM for the first experiment(Heart Rate Increasing) and in the second experiment, their heart rates varied from 157 to 70 BPM(Heart Rate Decreasing).

4.2.1 Experiment Setup

All experiments were set up under constant office fluorescent light. The lighting background was homogeneous and had no significant changes or variation. A Sony camcorder (HDR-PJ260VE) was used for the video recording purposes. All videos were recorded and sampled at 50 frames per second. All videos were recorded in 24-bit RGB (with 8 bits per channel). The camcorder was fixed at a position with a distance of about 0.60m from the subject's face. Viola et al. model used to detect the face region (Viola et al., 2001). The Region of Interest (ROI) is fixed at the area below eyes and above the upper lips of mouth in a video frame (Pursche et al., 2012). The obtained data were processed and analyzed offline using MATLAB R2016a.

In both experiments, the eight subjects were asked to cycle. In the first experiments, the eight subjects were asked to cycle at different speeds for about two minutes until significant changes of the subjects' heart rates were observed. The

camcorder then starts to capture their facial images for one minute. Throughout the video recordings, all subjects continue the cycling activity with minimum movement.

In the second experiment, the eight subjects were asked to cycle at high speed to raise their heart rates to a high level. When a significantly high level of heart rate is achieved, the subjects were asked to rest for one minute while the camcorder captures their facial images. The subject was requested to stay still with no motion during this period. As a reference, the instantaneous heart rates of each subject for both experiments were measured from Polar Heart Rate Monitor – Polar Team2 Pro (Schönfelder et al., 2011, Wallen et al., 2012).

4.2.2 First experiment: observed heart rates varying from low to high

In this experiment, the eight subjects' heart rates were measured, and the video duration is varied between 3 and 7 seconds. For each subject a total of 60 readings were obtained. A sliding window was used. The obtained results were compared to actual heart rate readings for each subject. Fig.4.1 shows the average Root Mean Square Error (RMSE) of all subjects using the proposed method and ICA. It can be seen that at short video duration from 3 to 4.5 seconds, the error is quite large when compared to video duration after 5 seconds for the proposed method. Fig. 4.2(a) – 4.2(h) shows the comparison of estimated heart rate readings with actual heart rate readings for all eight subjects using the proposed method and ICA based-method with the video duration varied between 4.5 and 7 seconds. For the 5 seconds video duration, it can be seen that the differences between the actual and estimated heart rates did not vary much for the proposed method as shown in Fig. 4.2(c). However, the same did not occur for the ICA based-method as shown in Fig. 4.2(d). In fact, quite a number of readings are very far from the actual readings. The RMSE using 5 seconds is 3.70 BPM while the Pearson coefficient is 0.97 for the proposed method. In the case of the ICA based-method, the RMSE is 14.36 BPM and 0.66 for the Pearson coefficient.

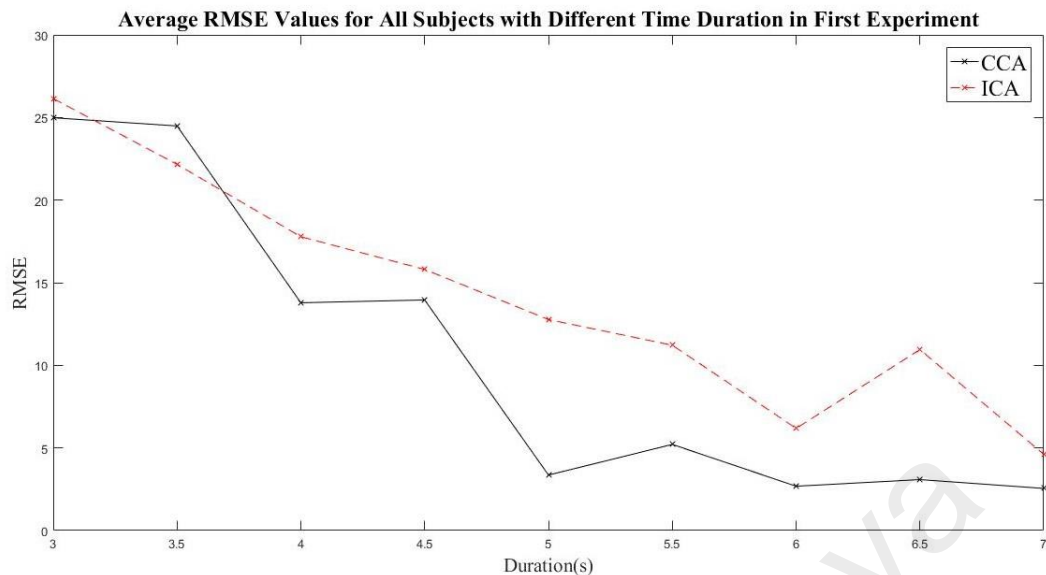


Figure 4.1: Average RMSE values for all eight subjects in first experiment with duration vary from 3s to 7s

The results for 6 seconds video duration as shown in Fig.4.2(e) and Fig.4.2(f) show a marginal improvement for the proposed method while a significant improvement for the ICA based-method respectively. In this case, the RMSE and Pearson coefficient for the proposed method and ICA based-method are 3.01 BPM and 0.98 and 7.39 BPM and 0.86 respectively. Despite a significant improvement in the RMSE score for ICA based-method, there are still some readings between the actual and estimated heart rate readings that are quite far apart as shown in Fig. 4.2(f). Further improvements can be observed for the ICA based-method when 7 seconds video duration is used as shown in Fig. 4.2(h). Still, there are some heart rate estimated readings that deviate from the actual readings, but that is not the case for the proposed method as shown in Fig. 4.2(g). The RMSE and Pearson coefficient for the proposed method and ICA based-method using 7 seconds are 2.97 BPM and 0.97 and 6.06 BPM and 0.9 respectively. For real-time application, the goal is to use a minimum video duration to compute the heart rate readings. These experimental results as shown in Fig. 4.2(a) to (h) show that acceptable results are obtain using the proposed method for a lower video duration than the ICA based-method. The results of the RMSE and Pearson coefficients for each subject for both CCA and ICA based-method for 5 seconds video

duration are shown in Table 4.1. As can be seen in Table 4.1, the lowest and the highest RMSE and Pearson coefficients using the proposed method are 1.20 BPM and 5.86 BPM and 0.59 and 0.99 respectively. However, ICA-based method gave 3.74 BPM and 22.27 BPM as the lowest and highest RMSE respectively while the lowest and highest Pearson coefficient scores were 0.11 and 0.88 respectively. From Table 4.1, it shows that CCA gives better results when compared to ICA. When the video duration is increased to 7 seconds, the RMSE and Pearson coefficient scores improved significantly for ICA based-method while the proposed method also shows some improvement as shown in Table 4.2. Details of comparison between CCA and ICA for each subject with duration vary between 4.5 to 7 –seconds were shown in Appendix A.

Table 4.1: The Result of the Heart Rate Readings for the first experiment (5s)

Subject	Heart Rate Value (BPM)		RMSE		Pearson correlation coefficient	
	Starting	Ending	CCA	ICA	CCA	ICA
1	98	111	3.16	3.74	0.70	0.72
2	83	96	4.30	4.05	0.59	0.64
3	84	122	3.20	11.25	0.98	0.73
4	95	130	2.11	18.83	0.99	0.34
5	101	124	5.86	19.35	0.83	0.11
6	93	144	1.78	8.98	0.99	0.88
7	112	139	1.20	13.70	0.99	0.37
8	111	132	5.26	22.27	0.95	0.12

Table 4.2: The Result of the Heart Rate Readings for the first experiment (7s)

Subject	Heart Rate Value (BPM)		RMSE		Pearson correlation coefficient	
	Starting	Ending	CCA	ICA	CCA	ICA
1	103	112	1.59	1.68	0.74	0.69
2	83	96	3.04	3.27	0.72	0.68
3	84	125	1.70	2.01	0.99	0.99
4	96	130	1.24	3.22	0.99	0.96
5	101	136	5.14	13.09	0.93	0.34
6	95	130	1.25	1.98	0.99	0.98
7	101	138	4.94	9.20	0.93	0.61
8	86	128	1.50	2.47	0.99	0.98

The detail readings of the 480 actual heart rate and from using CCA and ICA for eight subjects are shown in Figs. 4.2(a-h) for the first experiment. Figs. 4.2(a) and 4.2(b) show the comparison results of the actual heart rate and those obtained using CCA and ICA for 4.5 seconds respectively. It can be seen from those Figures that the accuracy whether using CCA or ICA is about the same. This illustrates that the time used in analyzing the obtained data for both cases is too short.

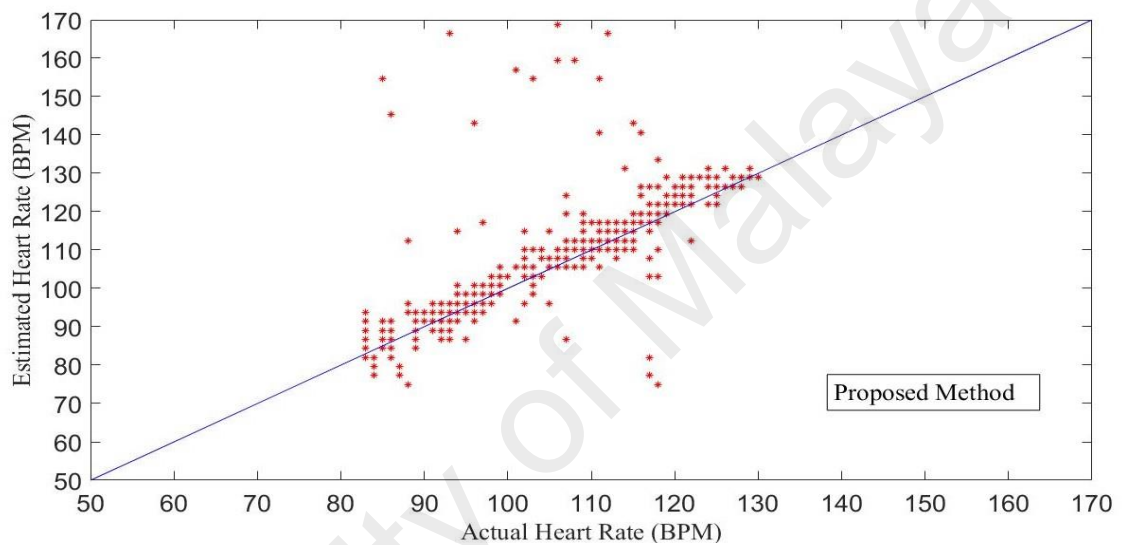


Figure 4.2(a): Comparison between actual heart rate readings and from the proposed method in the first experiment for all eight subjects for 4.5 seconds

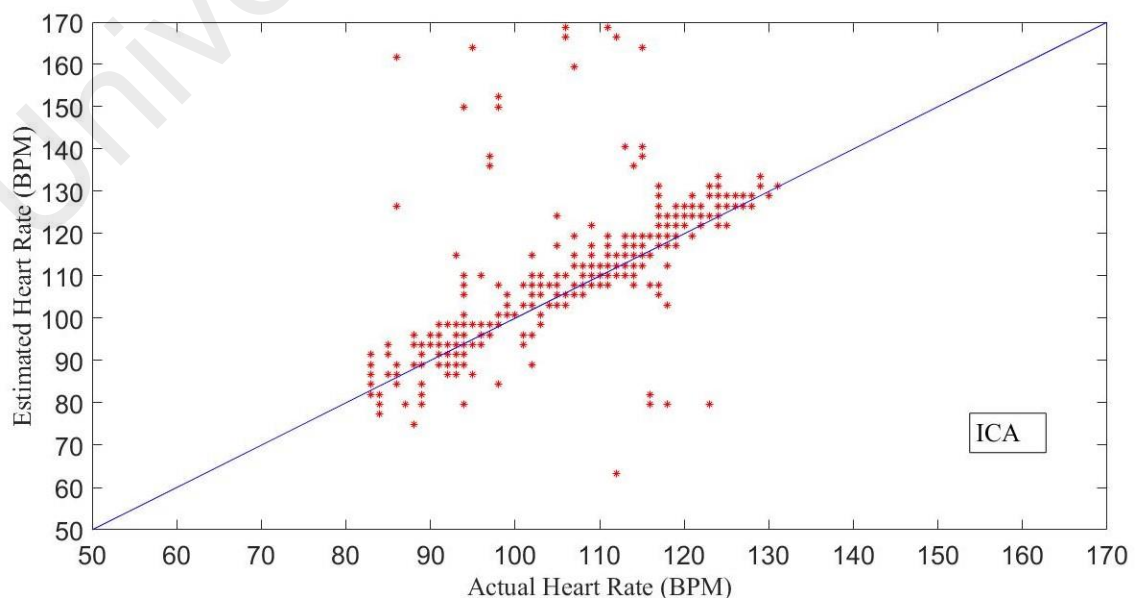


Figure 4.2(b): Comparison between actual heart rate readings and from ICA in the first experiment for all eight subjects for 4.5 seconds.

However, better results were obtained when the time was increased to 5 seconds as shown in Figure 4.2 (c). As can be seen in that Figure the actual hearts rate readings and from the proposed method are very close to the desired straight line. The same cannot be said when using ICA as shown in Figure 4.2(d). As can be seen in the Figure, there are quite a number of incorrect readings between the actual and those obtained using ICA.

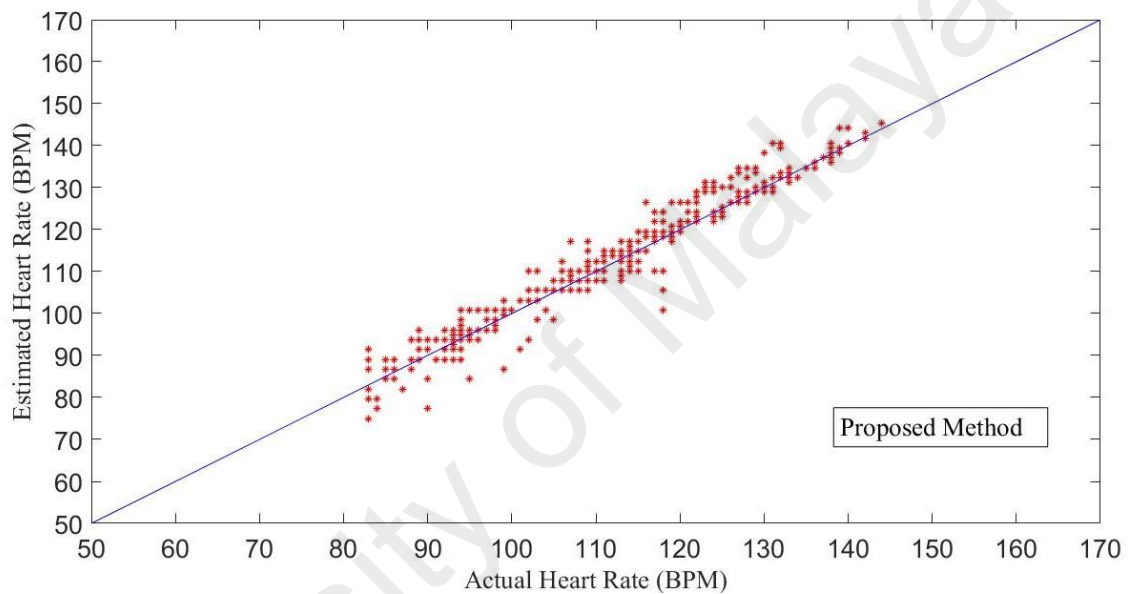


Figure 4.2(c): Comparison between actual heart rate readings and from the proposed method in the first experiment for all eight subjects for 5.0 seconds.

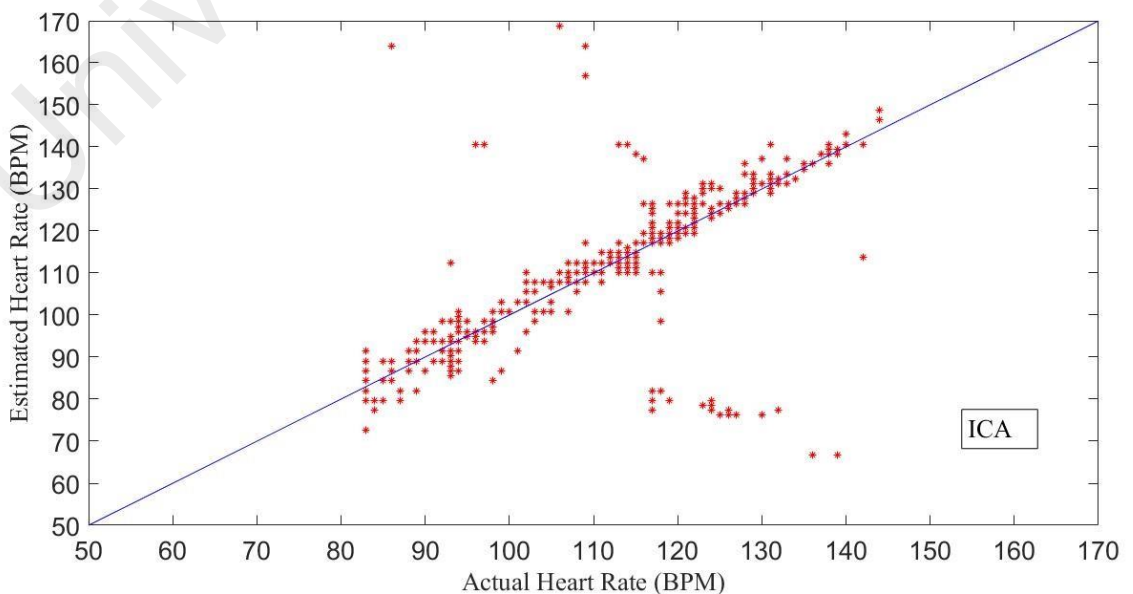


Figure 4.2(d): Comparison between actual heart rate readings and from ICA in the first experiment for all eight subjects for 5.0 seconds.

The time was further increased from 5 seconds to 6 seconds to see if better accuracies can be obtained for the proposed method as well as the method using ICA. Figures 4.2 (e) and (f) show the results. The distribution of the readings is much closer to the straight line for the proposed method as shown in Figure 4.2(e). Though the results for the ICA method have improved but still there are a few readings away from the straight line.

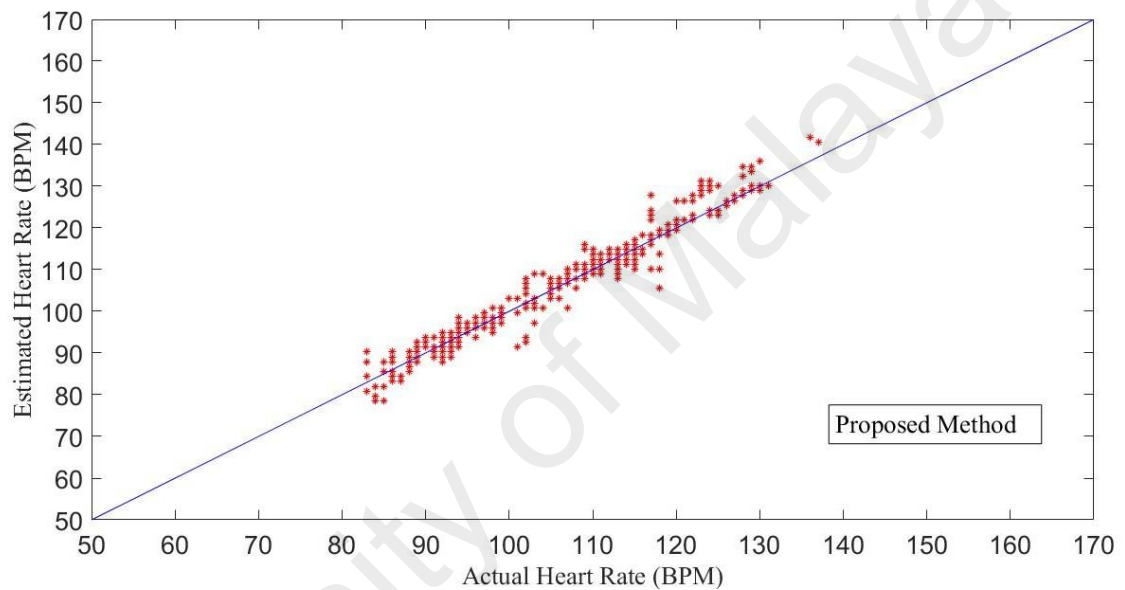


Figure 4.2(e): Comparison between actual heart rate readings and from the proposed method in the first experiment for all eight subjects for 6.0 seconds.

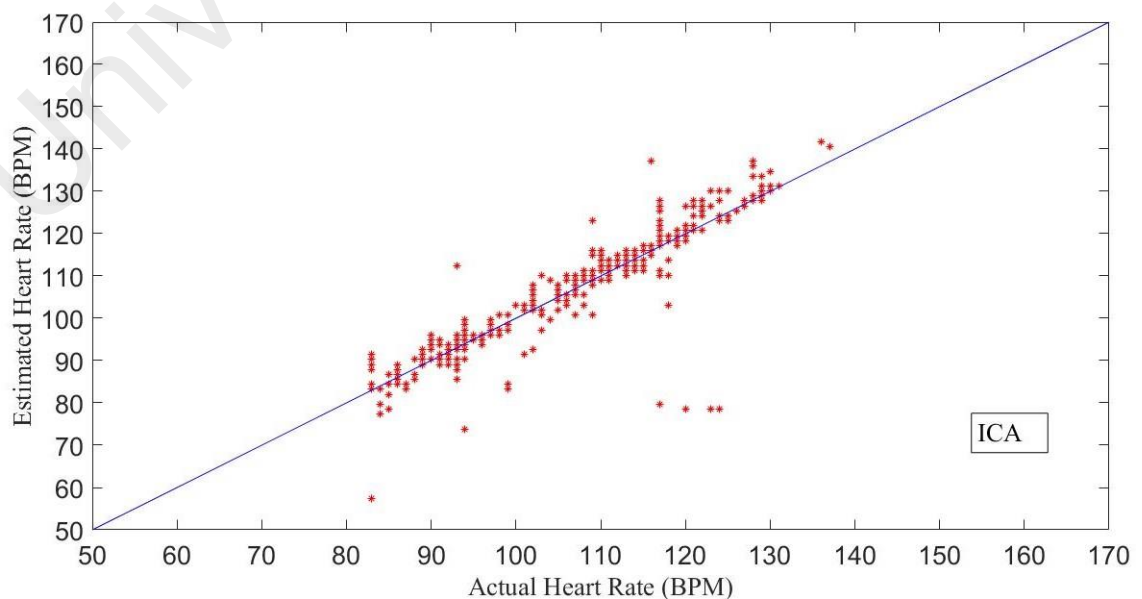


Figure 4.2(f): Comparison between actual heart rate readings and from ICA in the first experiment for all eight subjects for 6.0 seconds.

The last test for experiment 1 was that the time duration was increased to 7 seconds and the results are shown in Figures 4.2(g) and 4.2(h). The results of the proposed method and the ICA method are shown in Fig. 4.2(g) and Fig. 4.2(h) respectively. Notice that the results obtained for the proposed method as shown in Fig. 4.2(g) is almost similar to the ones obtained when the time duration was 5 seconds and 6 seconds. Though the results using ICA method has improved when compared to the earlier time durations, still there are few readings away from the straight line.

The detail readings of each subject for experiment 1 are given in Appendix A. Besides that the Pearson's correlation coefficient between the proposed method and ICA method for each subject for 4.5 seconds to 7 seconds is also given in Appendix A.

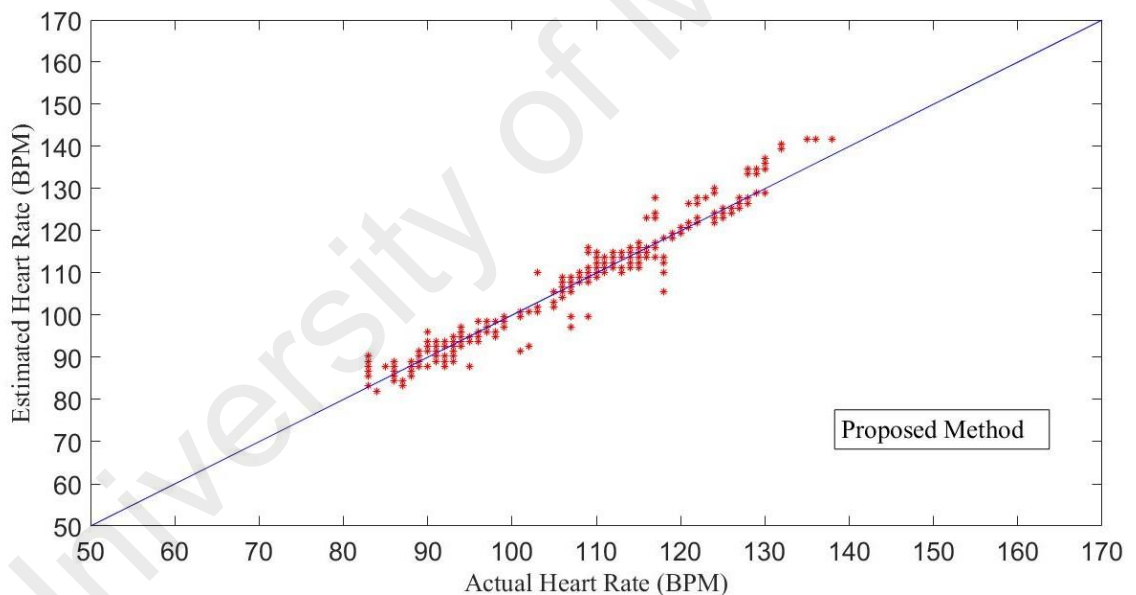


Figure 4.2(g): Comparison between actual heart rate readings and the proposed method in the first experiment for all eight subjects for 7 seconds.

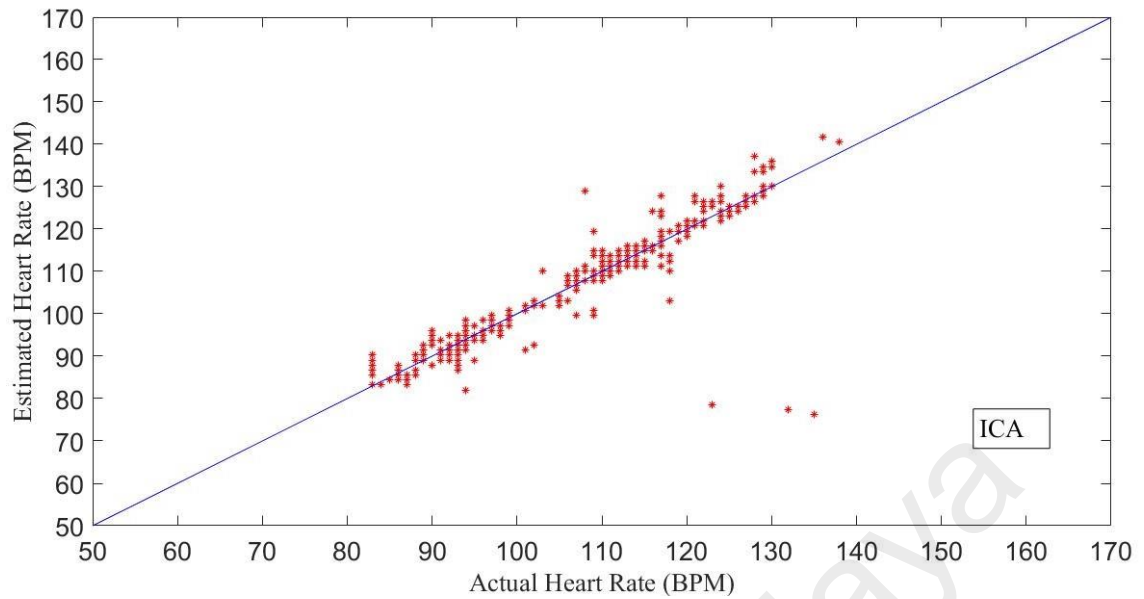


Figure 4.2(h): Comparison between actual heart rate readings and from ICA in the first experiment for all eight subjects for 7 seconds.

4.2.3 Second experiment: observed heart rates varying from high to low

In this experiment, the eight subjects' heart rates were decreasing. Just as in the first experiment, the video duration was varied between 3 and 7 seconds. Fig.4.3 shows the average RMSE of all subjects using the proposed method and ICA. It can be seen that at short video duration from 3 to 4.5 seconds, the error is quite large when compared to video duration after 5 seconds for the proposed method. Fig. 4.4 shows the comparison of estimated heart rate readings with actual heart rate readings for all eight subjects from 4.5 to 7 seconds. Notice the estimated heart rates between the estimated and the actual are quite close for the proposed method for a 5 seconds video duration as shown in Fig. 4.4(c). The RMSE for the 5 seconds video duration is 2.33 BPM while the Pearson coefficient is 0.99 for the proposed method. For ICA based-method, there are quite a number of readings that varied significantly between the estimated and the actual heart rate readings. As the video duration increases to 7 second, the number of heart rate readings between the estimated and actual does not vary much for both the proposed and the ICA based-method.

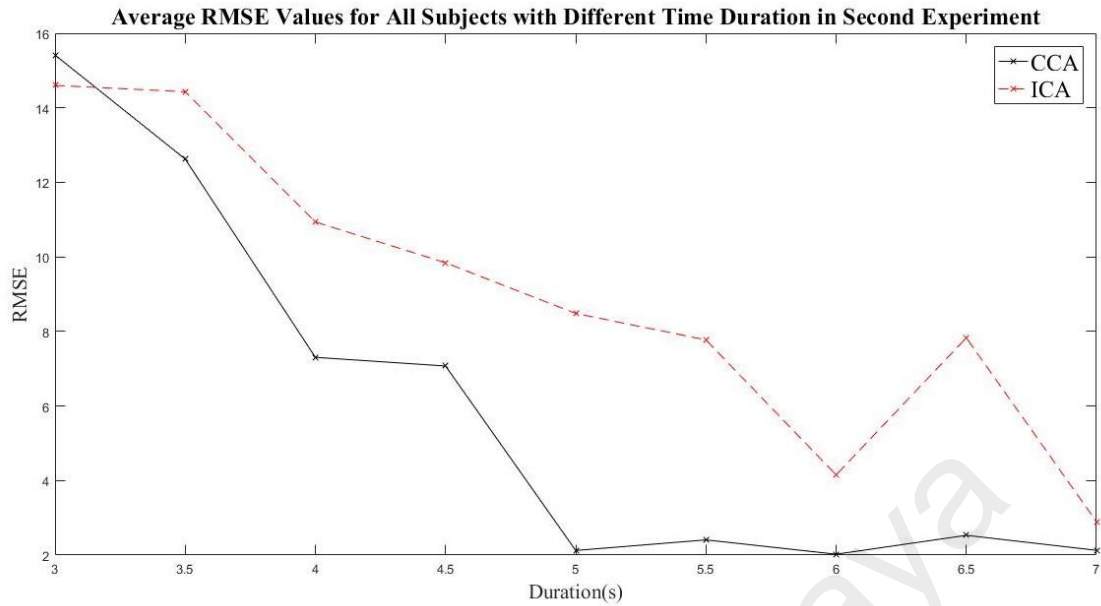


Figure 4.3: Average RMSE values for all eight subjects in second experiment with duration vary from 3s to 7s

Table 4.3: Summary of heart rate readings results in the second experiment (5s)

Subject	Heart Rate Value (BPM)		RMSE		Pearson correlation coefficient	
	Starting	Ending	CCA	ICA	CCA	ICA
1	115	97	1.40	2.78	0.96	0.90
2	94	71	2.02	2.03	0.96	0.97
3	153	121	1.39	1.64	0.99	0.98
4	145	128	3.75	10.67	0.75	0.29
5	151	116	2.58	13.64	0.96	0.67
6	153	121	1.64	1.88	0.99	0.99
7	151	115	1.87	13.21	0.98	0.51
8	145	126	2.92	16.22	0.86	0.31

Table 4.4: Summary of heart rate readings results in the second experiment (7s)

Subject	Heart Rate Value (BPM)		RMSE		Pearson correlation coefficient	
	Starting	Ending	CCA	ICA	CCA	ICA
1	115	97	1.62	1.93	0.97	0.96
2	94	71	1.50	1.88	0.98	0.97
3	153	121	2.28	2.41	0.99	0.99
4	145	126	3.21	5.32	0.84	0.70
5	153	121	1.89	2.09	0.99	0.99
6	151	114	1.43	1.90	0.99	0.98
7	144	126	2.18	2.23	0.90	0.90
8	151	114	1.88	2.31	0.99	0.99

Table 4.3 shows the results of the RMSE and Pearson coefficient for the eight subjects using the proposed method and ICA based-method for a 5 seconds video duration. It can be seen in Table 4.3 the highest RMSE is 3.75 BPM while the lowest RMSE is 1.39 BPM for the proposed method. However, the RMSE highest and lowest scores for ICA based-method is 16.22 BPM and 1.64 BPM respectively. When the video duration increases to 7 seconds, the RMSE scores decrease significantly for ICA based-method and also improvements are seen for the proposed method as shown in Table 4.4. Details of comparison between CCA and ICA for each subject with duration vary between 4.5 to 7 –seconds were shown in Appendix B.

Similar to the first experiment, the detail readings of the 480 actual heart rate and from using CCA and ICA for eight subjects are shown in Figs. 4.4(a-h) for the second experiment. Figs. 4.4(a) and 4.4(b) show the comparison results of the actual heart rate and those obtained using CCA and ICA for 4.5 seconds respectively. It can be seen from those Figures that the accuracy whether using CCA or ICA is about the same. There are some readings that are away from the straight line. This indicates that the time used in analyzing the obtained data for both cases is too short.

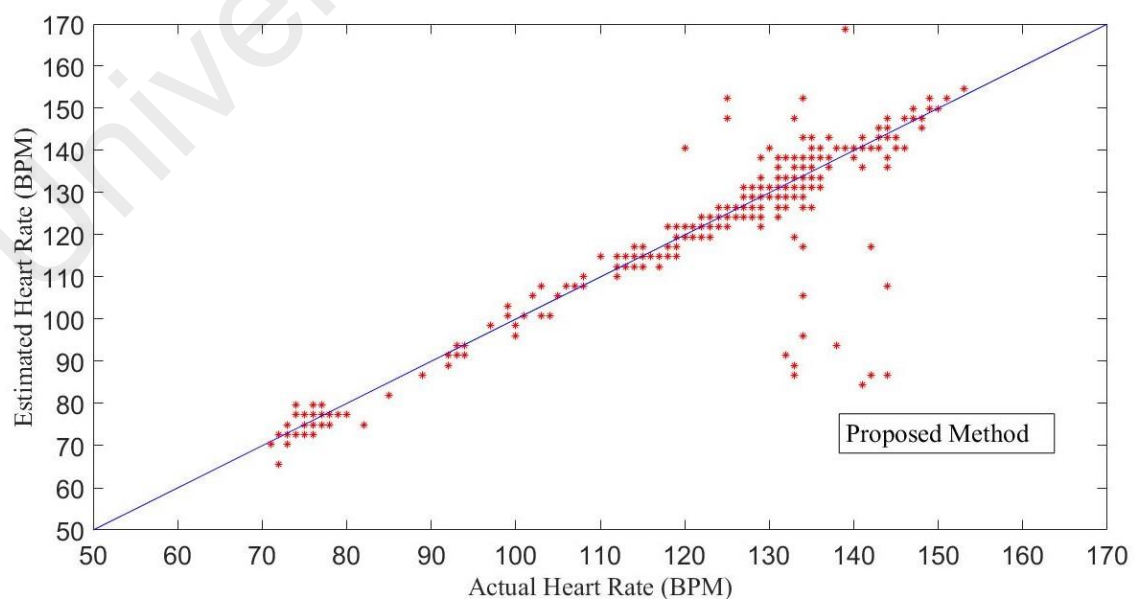


Figure 4.4(a): Comparison between actual heart rate readings and the proposed method in the second experiment for all eight subjects for 4.5 seconds.

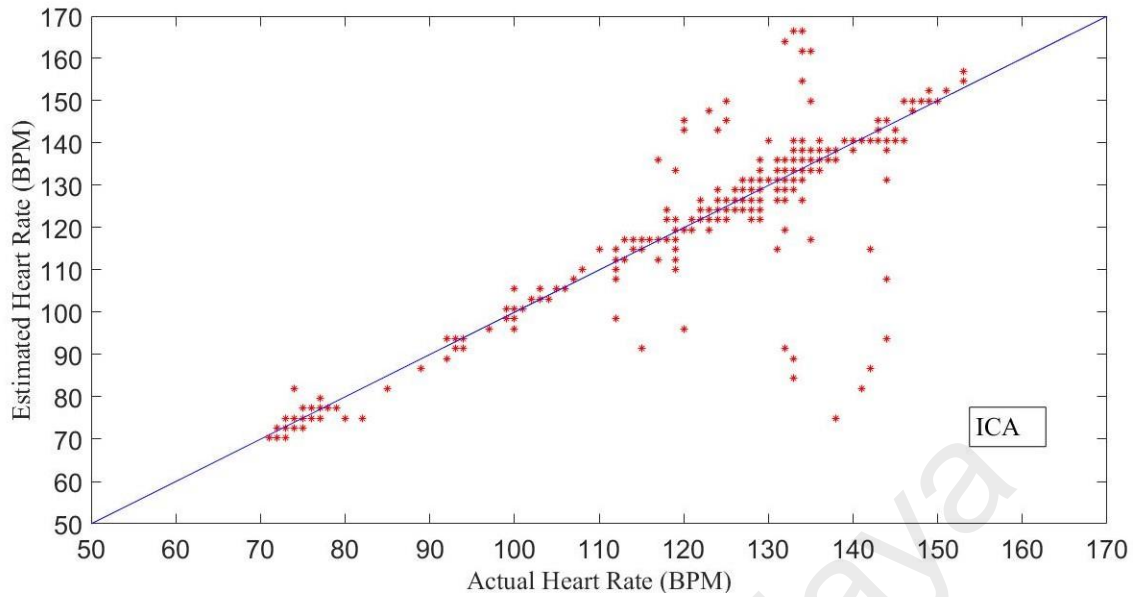


Figure 4.4(b): Comparison between actual heart rate readings and the ICA method in the second experiment for all eight subjects for 4.5 seconds.

When the time duration was increased to 5 seconds better accuracy results were obtained as shown in Figure 4.4 (c). As can be seen in that Figure the actual heart rate readings of the proposed method are very close to the desired straight line. When compared to experiment 1 results for 5 seconds, the accuracy of the results is better in the second experiment. This is because the subject does not have to cycle and hence less motion was involved during the entire duration. However the ICA method as shown in Figure 4.4(d) improved compared to same time duration for experiment 1, there were still some inaccurate results. Here, it can be seen some of the readings stray away from the desired straight line.

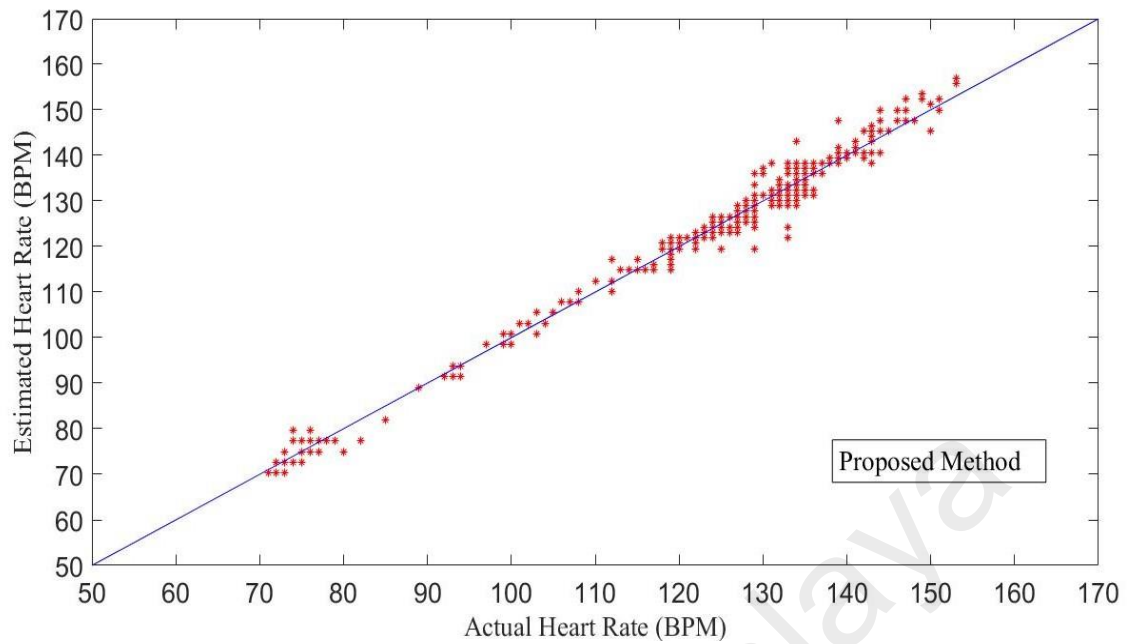


Figure 4.4(c): Comparison between actual heart rate readings and the proposed method in the second experiment for all eight subjects for 5.0 seconds.

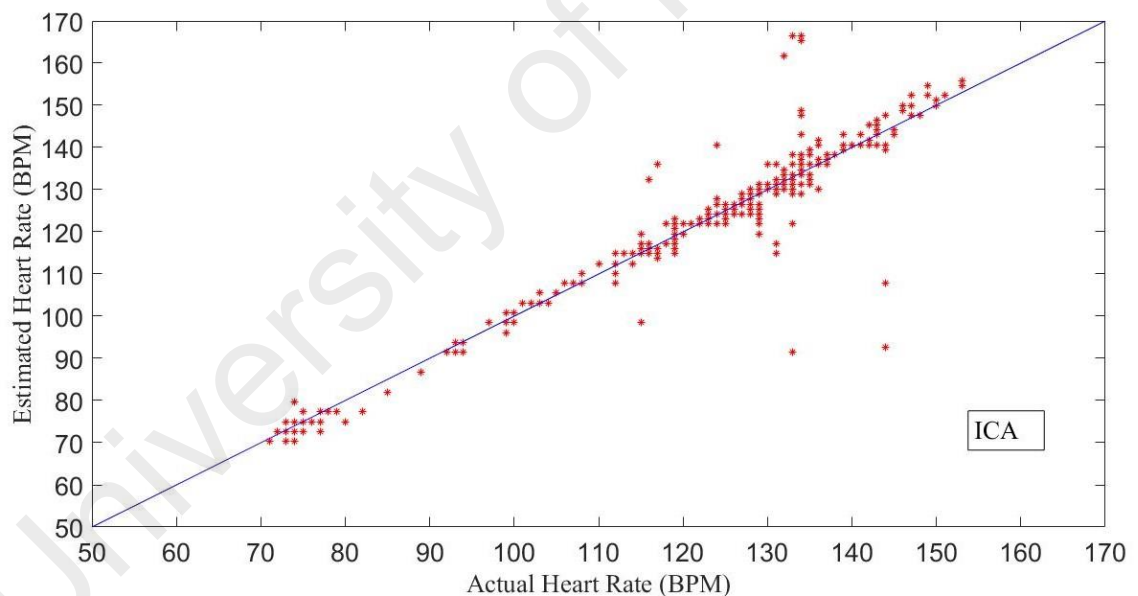


Figure 4.4(d): Comparison between actual heart rate readings and the ICA method in the second experiment for all eight subjects for 5.0 seconds.

The time duration was further increased from 5 seconds to 6 seconds to see if better accuracies can be obtained for the proposed method and the ICA method as shown in Figures 4.4 (e) and (f). As can be seen in Figure 4.4(e), the readings are much closer to the straight line for the proposed method. The accuracies between the actual readings and the proposed method in some cases were almost the same. Though the

results for the ICA method have improved but still there are a few readings away from the straight line.

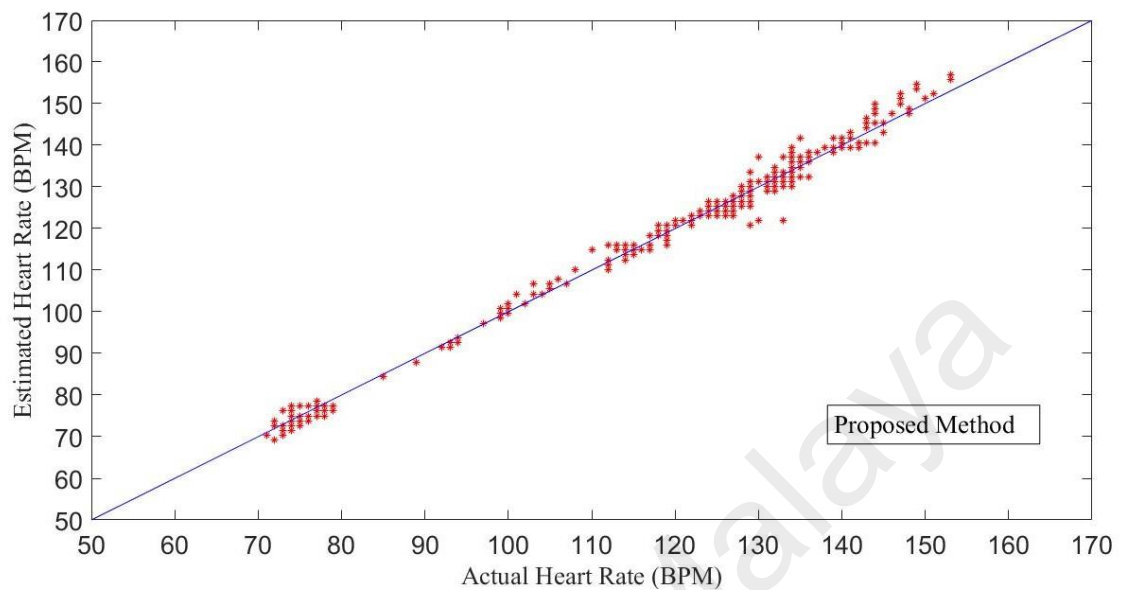


Figure 4.4(e): Comparison between actual heart rate readings and the proposed method in the second experiment for all eight subjects for 6 seconds.

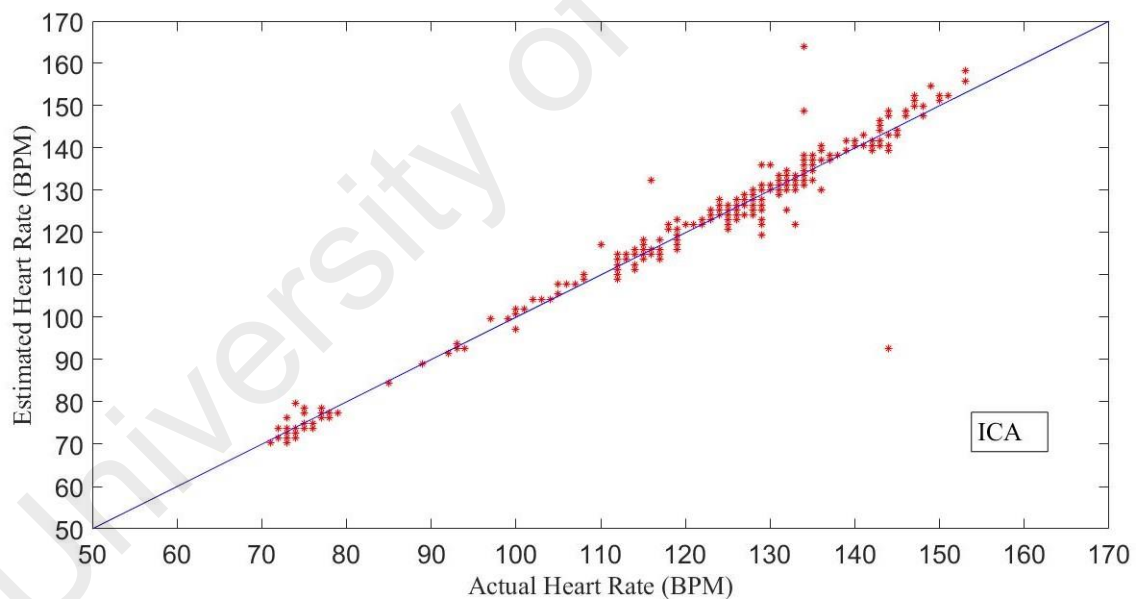


Figure 4.4(f): Comparison between actual heart rate readings and the ICA method in the second experiment for all eight subjects for 6 seconds.

The time duration was again increased to 7 seconds and the results for the proposed method and ICA method are shown in Figures 4.4(g) and 4.4(h) respectively. It can be seen from these Figures that the results obtained for the proposed method show very little difference between the actual readings and the results computed using the proposed method. Notice that the results obtained for the proposed method as shown in

Fig. 4.4(g) is almost similar to the ones obtained when the time duration was 5 seconds and 6 seconds. Since there is not much difference using a shorter duration is preferred. Though the results using ICA method has improved when compared to the earlier time durations, there are still few readings away from the straight line.

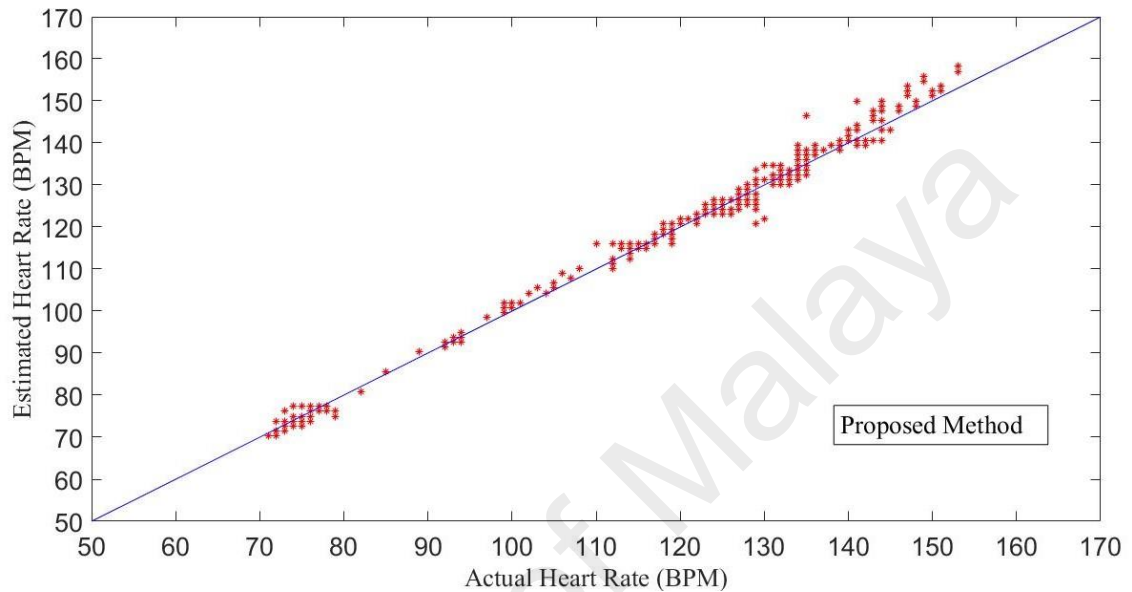


Figure 4.4(g): Comparison between actual heart rate readings and the proposed method in the second experiment for all eight subjects for 7 seconds.

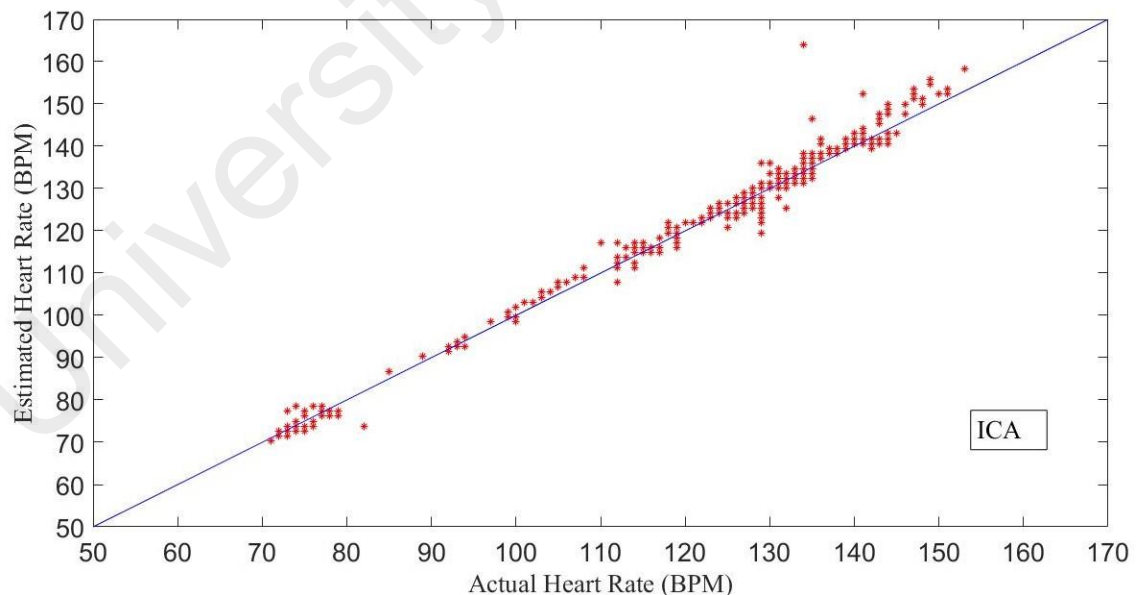


Figure 4.4(h): Comparison between actual heart rate readings and the ICA method in the second experiment for all eight subjects for 7 seconds.

The detail readings of each subject for experiment 2 are given in Appendix B. In addition to that, the Pearson's correlation coefficient between the proposed method and ICA method for each subject for 4.5 seconds to 7 seconds is also given in Appendix B.

4.3 Distance between the subject and video camera

By increasing the distance between the subject and video camera, the high-quality resolution is lost thereby affecting the accuracy of the heart rate estimation. In this study, two experiments were carried out to examine the impact of varying the distance between the subject and the video camera and to its heart rate estimation. In the first experiment, the distance between the subject and video camera was varied with a fixed duration. The distance was varied between 30cm and 200cm with a fixed duration of 5 and 8 seconds. In the second experiment, the duration was varied between 3 and 9 seconds with a fixed distance of 50cm and 100cm. Four subjects took part in the experiments.

4.3.1 Varying distance with fixed video duration

All experiments followed the setup described in section 4.1.1. The subject was seated on a chair facing the video camera with an initial distance of 30cm and was recorded for 60 seconds while his/her instantaneous heart rate reading was recorded simultaneously. The subject was requested to stay still with no motion. Viola et al. model used to detect the face region (Viola et al., 2001). The obtained data were processed and analyzed offline using MATLAB R2013a. The experiments were repeated by increasing the distance 10cm for each case until the final distance reaches 200cm. A total of 18 sets of videos and heart rate readings were captured for each subject. Four subjects' heart rates were measured, and they varied from 62 BPM to 90 BPM. A 5-second video clip was used in each case. The obtained results were compared to actual heart rate readings for each subject. This study also looks into the accuracy of the heart rate estimation when the duration is increased from 5-seconds to 8-seconds. Tables 4.5 and 4.6 show the Root Mean Square Error (RMSE) for all four subjects with

distance vary from 30cm to 200cm for both fixed duration of 5-seconds and 8-seconds respectively.

The error rates are much lower for 8-seconds duration when compared to 5-seconds duration. The results for both 5-seconds and 8-seconds duration gave the lowest scores when the distance was 50 cm. More details of the average error rates obtained from the differences between the estimated heart rates and actual heart rates for four subjects are shown using Box-Plot Graph in Figures 4.5 and 4.6. Each box in the Figures 4.5 and 4.6 indicate the average of the errors of the four subjects combined. In the experiment where varying the distance up to 120cm with fixed duration 5-seconds showed that acceptable error rates between the actual and computed method are observed and 130cm for fixed duration of 8-seconds.

Table 4.5: RMSE values for a distance varying from 30cm to 200cm with 5-seconds duration

Distance (cm)	RMSE with 5-seconds duration			
	S1	S2	S3	S4
30	1.07	4.20	3.32	1.34
40	1.80	1.78	4.41	3.99
50	2.45	2.19	3.02	2.75
60	1.62	3.76	2.23	1.95
70	2.07	2.51	5.39	1.12
80	2.19	1.84	3.16	5.06
90	2.13	1.64	2.70	1.61
100	1.74	1.95	3.65	2.46
110	1.53	7.04	7.04	0.95
120	1.48	3.44	2.43	6.48
130	36.47	7.85	3.77	5.40
140	4.15	3.50	56.65	2.77
150	36.71	1.27	50.51	2.53
160	7.01	1.58	64.64	1.78
170	60.36	2.48	7.79	3.47
180	2.38	1.50	10.69	20.26
190	16.98	4.30	29.42	8.82
200	66.37	3.01	10.56	34.11

Table 4.6: RMSE values for distance varying from 30cm to 200cm with 8-seconds duration

Distance (cm)	RMSE with 8-seconds duration			
	S1	S2	S3	S4
30	0.82	3.93	2.49	0.65
40	1.38	1.22	4.11	1.60
50	1.70	1.57	3.89	0.90
60	1.53	1.06	1.68	1.01
70	0.90	2.08	5.97	0.60
80	1.48	1.81	5.68	1.23
90	1.35	1.10	3.65	1.33
100	1.77	1.33	2.25	1.24
110	1.26	3.91	8.72	0.82
120	1.51	3.76	2.12	15.69
130	2.33	4.80	3.31	1.61
140	4.04	3.81	43.04	1.73
150	3.89	1.08	1.34	1.57
160	44.50	1.30	26.28	0.74
170	78.57	1.66	3.71	2.05
180	1.39	1.63	1.65	34.90
190	1.42	2.32	3.46	11.59
200	2.46	1.12	11.84	22.11

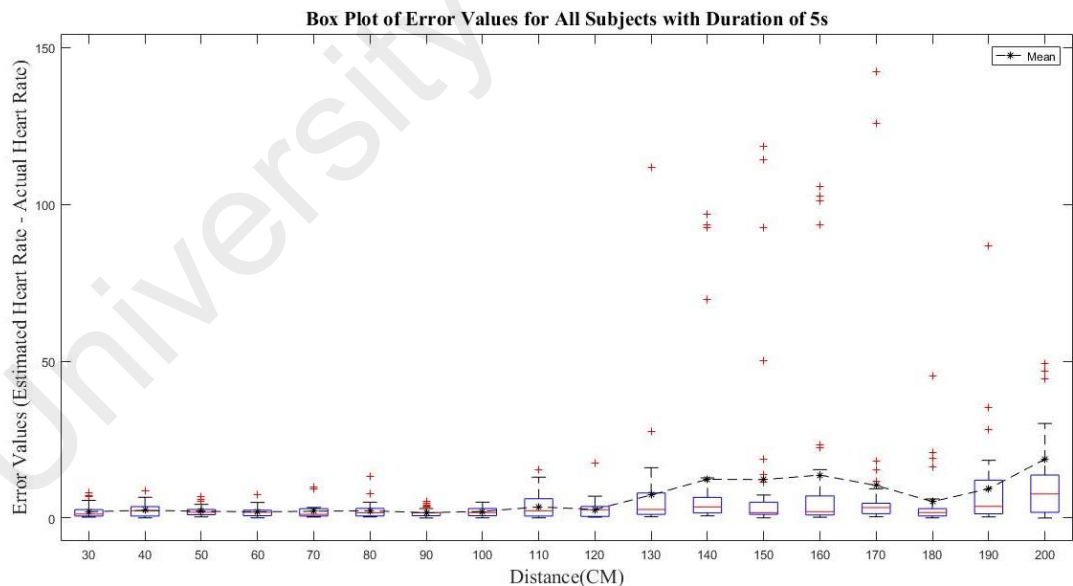


Figure 4.5: Box-Plot Graph of error values for all subjects with a duration time of 5 seconds

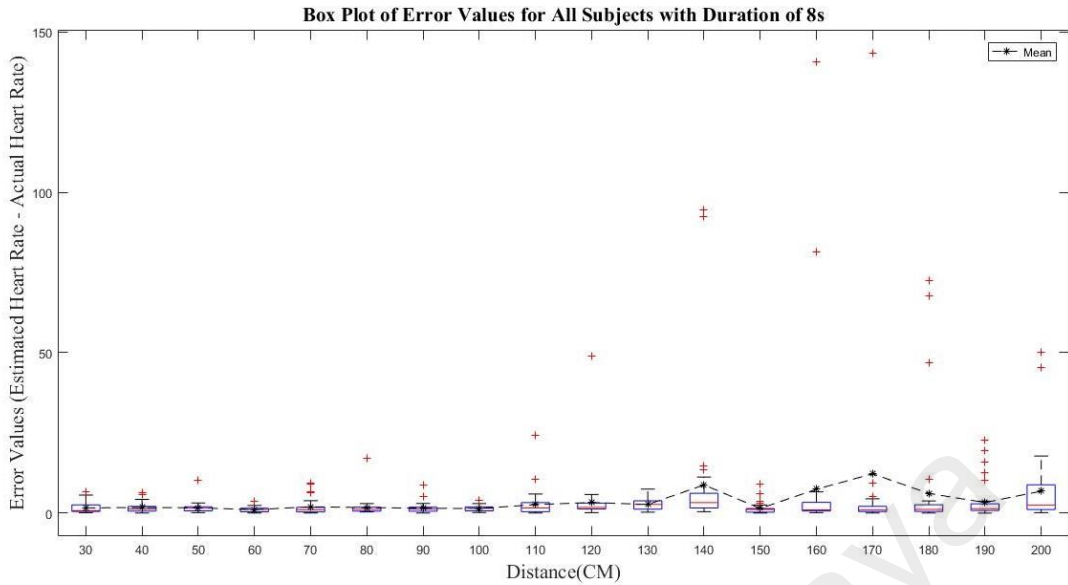


Figure 4.6: Box-Plot Graph of error values for all subjects with a duration time of 8 seconds

4.3.2 Fixed distance with varying video duration

The same four subjects from previous experiments were involved in this experiment. The same set-up as in the previous experiments was used except in this case the distance is fixed at 50 cm and 100 cm. The video frames used to analyze the data were varied from 3-seconds to 9-seconds. The same integrated CCA method is shown in Figure 3.1 was used to obtain the estimated heart rate readings. Tables 4.7 and 4.8 show the RMSE values for the four subjects with varying video duration for a fixed distance at 50cm and 100cm respectively. The results in Table 4.7 show that beyond 4-second duration gave acceptable errors between the estimated and actual readings. Similar observations can be seen in Table 4.8 where in this case, the video duration beyond 5-second produces acceptable error rates. More details of the errors are shown using Box-Plot graph as shown in Figures 4.7 and 4.8 for the distance 50cm and 100cm respectively. In this experiment where the video duration is varied with a fixed distance of 50cm and 100cm showed that beyond 5-second video duration gave acceptable error rates for both fixed distances.

Table 4.7: RMSE values for varying duration time at distance of 50cm

Time Duration (s)	RMSE at distance of 50cm			
	S1	S2	S3	S4
3	4.02	2.63	5.45	17.99
4	2.54	1.70	5.61	2.71
5	2.53	2.19	3.02	2.75
6	2.13	1.87	3.03	2.04
7	1.97	1.73	2.64	1.29
8	1.70	1.57	3.89	0.90
9	1.67	1.57	3.16	0.59

Table 4.8: RMSE values for varying duration time at distance of 100cm

Time Duration (s)	RMSE at distance of 100cm			
	S1	S2	S3	S4
3	4.32	3.18	46.23	12.13
4	2.46	1.70	11.42	6.21
5	1.74	1.62	3.65	2.46
6	1.48	1.04	1.11	1.64
7	1.90	1.22	0.79	1.30
8	1.77	1.28	0.99	1.18
9	1.63	1.14	0.89	1.17

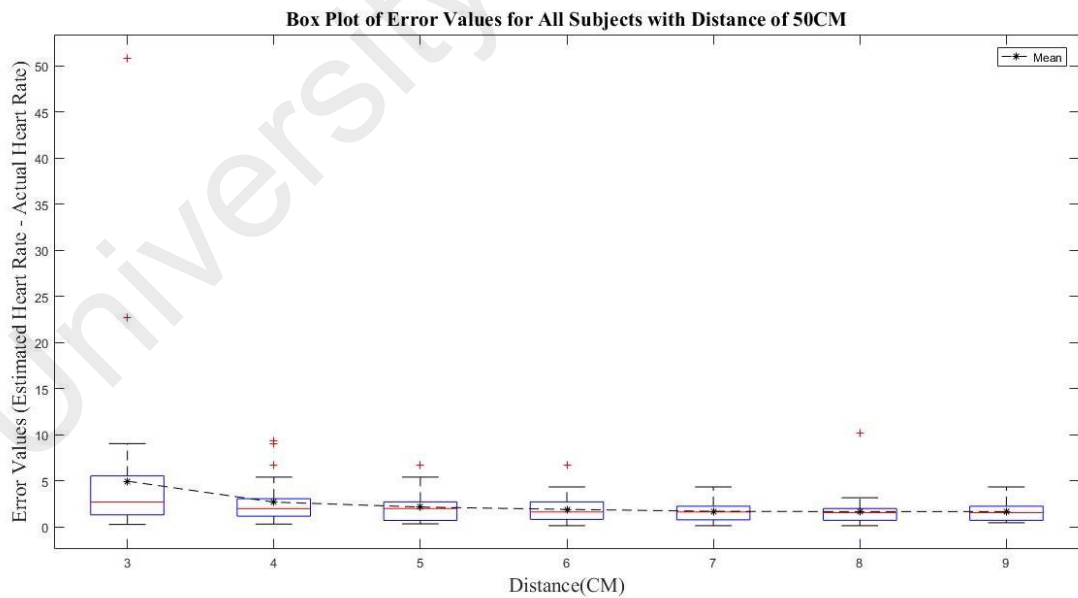


Figure 4.7: Box-Plot Graph of error values for all subjects with a distance of 50cm

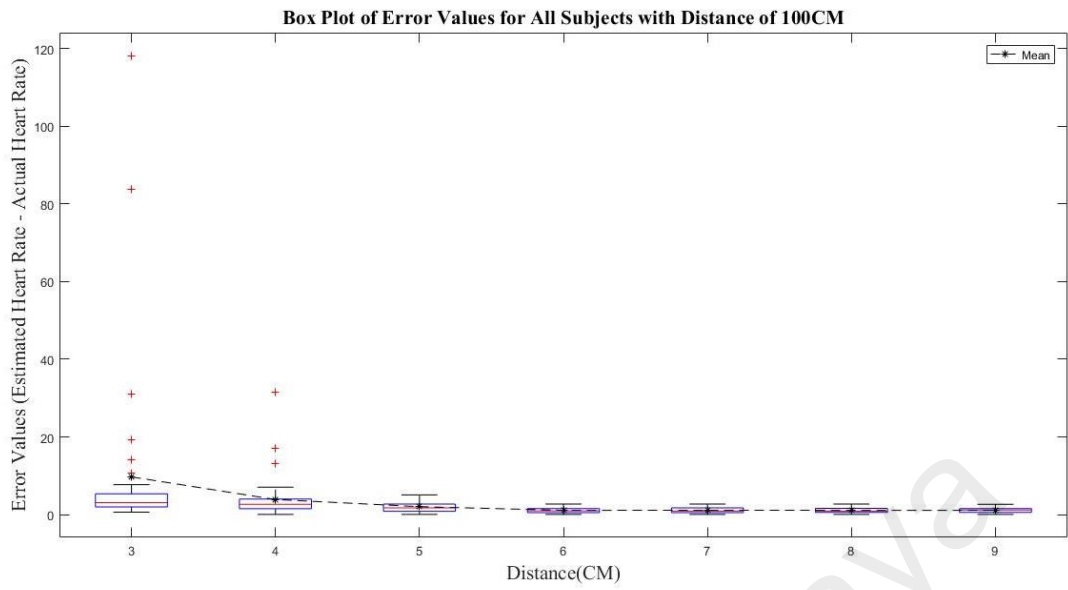


Figure 4.8: Box-Plot Graph of error values for all subjects with a distance of 100cm

University of Malaysia

CHAPTER 5: CONCLUSION

A new method to estimate heart rate from the video was presented. In this study, heart rate estimation from the video can be obtained by using canonical component analysis method. The canonical component analysis determines the relationship between two sets of variables by computing their correlation values. Since the heart rate signals remain almost unchanged or very little changed in a second, CCA can be used to give maximum correlation values. By using blind source separation by Canonical Component Analysis method, the heart rate signals can be estimated from videos. In this thesis, all experiments were conducted with constant office fluorescent light, hence the lighting background was homogeneous and had no significant changes or variation.

Two experiments of eight subjects for each experiment has been carried out to examine the effectiveness of the proposed method. In both experiments, the eight subjects were asked to cycle. In the first experiment, the eight subjects were asked to cycle at different speeds for about two minutes until significant changes of the subjects' heart rates were observed. The camcorder then starts to capture their facial images for one minute. Throughout the video recordings, all subjects continue the cycling activity with minimum movement.

In the second experiment, the eight subjects were asked to cycle at high speed to raise their heart rates to a high level. When a significantly high level of heart rate is achieved, the subjects were asked to rest for one minute while the camcorder captures their facial images. The subject was requested to stay still with no motion during this period. As a reference, the instantaneous heart rates of each subject for both experiments were measured from Polar Heart Rate Monitor – Polar Team2 Pro (Schönfelder et al., 2011, Wallen et al., 2012). From these experiments the RMSE was 3.70 BPM and 2.33 BPM for the first and second experiments respectively.

In the second part of this study, we also examine the impact of varying the distance between the subject and the video camera and also fixing the distance but varying the video duration. By increasing the distance between the subject and video camera, the high-quality resolution is lost thereby affecting the accuracy of the heart rate estimation. Two experiments were carried out to examine the impact of varying the distance between the subject and the video camera and to its heart rate estimation. In the first experiment, the distance between the subject and video camera was varied with a fixed duration. The distance was varied between 30cm and 200cm with a fixed duration of 5 and 8 seconds. In the second experiment, the duration was varied between 3 and 9 seconds with a fixed distance of 50cm and 100cm. Four subjects took part in the experiments. In the experiment where varying the distance up to 120cm with fixed duration 5-seconds showed that acceptable error rates between the actual and computed method are observed and 130cm for fixed duration of 8-seconds. In the last experiment where the video duration is varied with a fixed distance of 50cm and 100cm showed that beyond 5-second video duration gave acceptable error rates for both fixed distances.

There are still many possibilities to extend and improve the works presented in this thesis. First, the experiment can be conducted with variation of illumination. The variation in illumination conditions is a very important factor affecting video based heart rate measurement. Therefore, an experiment with variation of illumination can be conducted to investigate the impact of variation of illumination on the accuracy of the results.

One of the disadvantages of using CCA to estimate the heart rate reading is long computing time. Even with a short duration of video frame, to estimate heart rate reading from video sequence by using CCA still involves many pre-processing steps, hence causing the long computing time. Further research on estimating heart rate

readings from video sequences still needed to be improved for it to be commercially acceptable.

Lastly, future work may be extended to the dynamic heart rate measurements from human skin other than face, for instance, wrist, arm, or palm. It is more practical if human heart rate can be obtained using any human skin images from video sequences.

University of Malaya

REFERENCES

- AlGhatrif, M., & Lindsay, J. (2012). A brief review: history to understand fundamentals of electrocardiography. *Journal of community hospital internal medicine perspectives*, 2(1), 14383.
- Allen, J., Hayat, A., & Raviv, G. . (1977). Reflection photoplethysmography of arterial-blood-volume pulses. *Medical and Biological Engineering and Computing*, 15(1), 22-31.
- Allen, J. (2007). Photoplethysmography and its application in clinical physiological measurement. *Physiological measurement*, 28(3), R1.
- Alzahrani, A. (2015). Preprocessing Realistic Video for Contactless Heart Rate Monitoring Using Video Amplification Methodologies (Doctoral dissertation). Carleton University Ottawa.
- Baig, M. M. (2010). Smart monitoring systems for alert generation during anaesthesia. (Doctoral dissertation). Auckland University of Technology.
- Bowmaker, J. K., & Dartnall, H. (1980). Visual pigments of rods and cones in a human retina. *The Journal of physiology*, 298(1), 501-511.
- Cardoso, J. F., & Souloumiac, A. (1993, December). Blind beamforming for non-Gaussian signals. In *IEE proceedings F (radar and signal processing)* (Vol. 140, No. 6, pp. 362-370). IET Digital Library.
- Cardoso, J. F. (1999). High-order contrasts for independent component analysis. *Neural computation*, 11(1), 157-192.
- Docampo, G. N., & Casas, P. (2012). Heart rate estimation using facial video information. *Escuela Técnica Superior de Ingenieros de Telecomunicaciones, Universita Polit ècnica de Catalunya*, 2012, 1-70.
- Finlayson, G. D., Drew, M. S., & Lu, C. (2004, May). Intrinsic images by entropy minimization. In *European conference on computer vision* (pp. 582-595). Springer, Berlin, Heidelberg.
- Garbey, M., Sun, N., Merla, A., & Pavlidis, I. (2007). Contact-free measurement of cardiac pulse based on the analysis of thermal imagery. *Ieee Transactions on Biomedical Engineering*, 54(8), 1418-1426.
- Gatto, R. G. (2009). Estimation of instantaneous heart rate using video infrared thermography and ARMA models. (Doctoral dissertation). University of Illinois at Chicago.
- Hamedani, K., Bahmani, Z., & Mohammadian, A. (2016) Spatio-temporal filtering of thermal video sequences for heart rate estimation. *Expert Systems with Application*, 54, pp.88-94.

- Hardoon, D. R., Szedmak, S., & Shawe-Taylor, J. (2004). Canonical correlation analysis: An overview with application to learning methods. *Neural computation*, 16(12), 2639-2664.
- Hertzman, A. B. (1938). The blood supply of various skin areas as estimated by the photoelectric plethysmograph. *American Journal of Physiology*, 124(2), 328-340.
- Humphreys, K., Ward, T., & Markham, C. (2007). Noncontact simultaneous dual wavelength photoplethysmography: a further step toward noncontact pulse oximetry. *Review of scientific instruments*, 78(4), 044304.
- Hyvärinen, A., & Oja, E. (2000). Independent component analysis: algorithms and applications. *Neural networks*, 13(4), 411-430.
- Jensen, J. N., & Hannemose, M. (2014). Camera-based Heart Rate Monitoring. Department of Applied Mathematics and Computer Science, DTU Computer, 17.
- Jonathan, E., & Leahy, M. (2010). Investigating a smartphone imaging unit for photoplethysmography. *Physiological Measurement*, 31(11), N79-N83.
- Kamal, A. A. R., Harness, J. B., Irving, G., & Mearns, A. J. (1989). Skin photoplethysmography—a review. *Computer methods and programs in biomedicine*, 28(4), 257-269.
- Kamshilin, A. A., Miridonov, S., Teplov, V., Saarenheimo, R., & Nippolainen, E. (2011). Photoplethysmographic imaging of high spatial resolution. *Biomedical Optics Express*, 2(4), 996-1006.
- Kumar, M., Veeraraghavan, A., & Sabharwal, A. (2015). DistancePPG: Robust non-contact vital signs monitoring using a camera. *Biomedical Optics Express*, 6(5), 1565-1588.
- Lee, T. W., Lewicki, M. S., & Sejnowski, T. J. (2000). ICA mixture models for unsupervised classification of non-Gaussian classes and automatic context switching in blind signal separation. *IEEE Transactions on Pattern Analysis and Machine Intelligence*, 22(10), 1078-1089.
- Liu, W., Ji, J., Chen, H., & Ye, C. (2014). Optimal color design of psychological counseling room by design of experiments and response surface methodology. *PloS one*, 9(3), e90646.
- M. Borga, H. Knutsson,(2001, June). A Canonical Correlation Approach to Blind Source Separation. Linköping University, Linköping, Sweden, Technical Report LiU-IMT-EX-0062, 2001.
- Mendelson, Y., & Ochs, B. D. (1988). Noninvasive pulse oximetry utilizing skin reflectance photoplethysmography. *IEEE Transactions on Biomedical Engineering*, 35(10), 798-805.
- Mosby's Medical Dictionary (8th ed.). (2009). St. Louis, MO: Mosby Elsevier.

- Nemati, Ebrahim & Deen, M.J. & Mondal, Tapas. (2012). A Wireless Wearable ECG Sensor for Long-Term Applications. *IEEE Communications Magazine*. 50. 36-43.
- Pavlidis, I., Dowdall, J., Sun, N., Puri, C., Fei, J., & Garbey, M. (2007). Interacting with human physiology. *Computer Vision and Image Understanding*, 108(1-2), 150-170.
- Poh, M. Z., McDuff, D. J., & Picard, R. W. (2010). Non-contact, automated cardiac pulse measurements using video imaging and blind source separation. *Optics Express*, 18(10), 10762-10774.
- Poh, M. Z., McDuff, D. J., & Picard, R. W. (2011). Advancements in Noncontact, Multiparameter Physiological Measurements Using a Webcam. *Ieee Transactions on Biomedical Engineering*, 58(1), 7-11.
- Procházka, A.; Schätz, M.; Vyšata, O.; Vališ, M.(2016) Microsoft kinect visual and depth sensors for breathing and heart rate analysis. *Sensors*, 16, pp. 996.
- Pursche, T., Krajewski, J., & Moeller, R. (2012). Video-based Heart Rate Measurement From Human Faces. 2012 Ieee International Conference on Consumer Electronics (Icce).
- P. Viola and M. Jones, Rapid object detection using a boosted cascade of simple features, in Proceedings of the IEEE Computer Society Conference on Computer Vision and Pattern Recognition, 2001 (IEEE, 2001), pp. 1511.
- Rattfalt, L., Ahlstrom, C., Berglin, L., Lindén, M., Hult, P., Ask, P., & Wiklund, U. (2006). A canonical correlation approach to heart beat detection in textile ECG measurements. Proceedings of ET 3rd International Conference MEDSIP 2006. *Advances in Medical, Signal and Information Processing*, 2006.
- Scalise, L., & Morbiducci, U. (2008). Non-contact cardiac monitoring from carotid artery using optical vibrocardiography. *Medical Engineering and Physics*, 30(4), 490-497.
- Schönfelder, M., Hinterseher, G., Peter, P., & Spitzenpfeil, P. (2011). Scientific comparison of different online heart rate monitoring systems. *International Journal of Telemedicine and Applications*, 2011,6.
- Shi, P., Peris, V. A., Echiadis, A., Zheng, J., Zhu, Y. S., Cheang, P. Y. S., & Hu, S. J. (2010). Non-contact Reflection Photoplethysmography Towards Effective Human Physiological Monitoring. *Journal of Medical and Biological Engineering*, 30(3), 161-167.
- Takano, C., & Ohta, Y. (2007). Heart rate measurement based on a time-lapse image. *Medical Engineering & Physics*, 29(8), 853-857.
- Tamura, T., Maeda, Y., Sekine, M., & Yoshida, M. (2014). Wearable photoplethysmographic sensors—past and present. *Electronics*, 3(2), 282-302.

- Tarvainen, M.P., Ranta-Aho, P.O., & Karjalainen, P. A. (2002). An advanced detrending method with application to HRV analysis. *IEEE Transactions on Biomedical Engineering*, 49(2), 172-175.
- Tsumura, N., Ojima, N., Sato, K., Shiraishi, M., Shimizu, H., Nabeshima, H., & Miyake, Y. (2003). Image-based skin color and texture analysis/synthesis by extracting hemoglobin and melanin information in the skin. *ACM Transactions on Graphics (TOG)*, 22(3), 770-779.
- Van Kampen, E. J., & Zijlstra, W. G. (1966). Determination of hemoglobin and its derivatives. In *Advances in clinical chemistry* (Vol. 8, pp. 141-187). Elsevier.
- Verkruyse, W., Svaasand, L. O., & Nelson, J. S. (2008). Remote plethysmographic imaging using ambient light. *Optics Express*, 16(26), 21434-21445.
- Vilhena, L., & Ramalho, A. (2016). Friction of human skin against different fabrics for medical use. *Lubricants*, 4(1), 6.
- Wallen, M. B., Hasson, D., Theorell, T., Canlon, B., & Osika, W. (2012). Possibilities and limitations of the polar RS800 in measuring heart rate variability at rest. *European Journal of Applied Physiology*, 112(3), 1153-1165.
- Wallet, B. C., & Davogustto, O. (2015). Integrating phase into the visualization of spectral decomposition attributes. *Interpretation*, 3(3), SS73-SS86.
- Weinman, J., Hayat, A., Raviv, & G. Reflection (1977) photoplethysmography of arterial-blood-volume pulses, *Medical and Biological Engineering and Computing*, 15, pp. 22-31.
- Wilson, S.F. (2012). C O N C E P T 15 Perfusion Definition(s) Scope and Categories.
- Wu, H. Y., Rubinstein, M., Shih, E., Guttag, J., Durand, F., & Freeman, W. (2012). Eulerian video magnification for revealing subtle changes in the world. *ACM Transactions on Graphics* 31(4), 1–8.
- Xu, S. C., Sun, L. Y., & Rohde, G. K. (2014). Robust efficient estimation of heart rate pulse from video. *Biomedical Optics Express*, 5(4), 1124-1135.
- Yu, Y. P.; Raveendran, P.; Lim, C. L. (2015) Dynamic heart rate measurements from video sequences. *Biomedical Optics Express*, 6, 2466-2480.
- Yu, Y. P.; Raveendran, P.; Lim, C. L.; Kwan, B. H. (2015) Dynamic heart rate estimation using principal component analysis. *Biomedical Optics Express*, 6, pp. 4610-4618.
- Yu, Y. P. (2016) Dynamic heart rate estimation using facial images from video sequences. (Doctoral dissertation). University of Malaya, Malaysia.
- Zheng, J., Hu, S., Chouliaras, V., & Summers, R. (2008, May). Feasibility of imaging photoplethysmography. In *BioMedical Engineering and Informatics, 2008. BMEI 2008. International Conference on* (Vol. 2, pp. 72-75). IEEE.

LIST OF PUBLICATIONS AND PAPERS PRESENTED

Ling, S. S.; Raveendran, P.; Yu, Y. P (2019) Dynamic Heart Rate Measurements from Video Sequences using Canonical Component Analysis. *Advances in Electrical and Computer Engineering*, 19(3), 41-48.

Ling, S. S.; Raveendran, P.; Yu, Y. P (2018). Video Based Heart Rate Estimation Using Facial Images from Video Sequences. In S.Y. Yurish (Eds.), *Advances in Optics: Reviews*, Vol. 3 (pp. 229-244). Spain: International Frequency Sensor Association (IFSA) Publishing

University of Malaya